

INTER-AMERICAN TROPICAL TUNA COMMISSION

100<sup>TH</sup> MEETING

Phoenix, Arizona (USA)

1-5 August 2022

DOCUMENT IATTC-100 INF-B

SOUTH EPO SWORDFISH BENCHMARK ASSESSMENT IN 2019

Carolina Minte-Vera, Mark N. Maunder, Haikun Xu, Juan Valero, Alexandre Aires-da-Silva

CONTENTS

EXECUTIVE SUMMARY .....	2
1. INTRODUCTION.....	4
1.1. BACKGROUND.....	4
2. CONCEPTUAL MODEL AND STOCK STRUCTURE ASSUMPTIONS .....	4
3. DATA .....	5
3.1. CATCHES .....	5
3.1.1. CATCH ESTIMATION .....	5
3.1.2. CATCH TRENDS.....	6
3.1.3. FISHERY DEFINITIONS .....	7
3.2. INDICES OF ABUNDANCE.....	8
3.3. COMPOSITION DATA .....	9
3.4. DATA WEIGHTING.....	9
4. REFERENCE MODELS.....	10
4.1. GENERAL MODEL STRUCTURE.....	10
4.2. SELECTIVITIES.....	10
4.3. MODELS BY HYPOTHESIS .....	10
5. RESULTS .....	11
5.1. INITIAL REFERENCE MODEL (MODEL 0).....	11
5.2. Models by hypothesis.....	12
5.3. Stock status.....	13
6. Discussion .....	15
6.1. Increase in PRODUCTIVITY.....	16
6.2. Increase in availability .....	17
6.3. Increase in productivity and availability .....	18
6.4. Increase in connectivity .....	18
7. Conclusion.....	18
8. Research recommendations .....	19
9. Acknowledgements .....	20
10. References .....	20
11. Appendix 1 . Catch estimation.....	54
12. Appendix 2. early model.....	54
Appendix 3 -Estimates of catchability by year for indices of abundance in model 2 .....	56
Appendix 4. Fits to the indices of abundance of the models according to the hypotheses.....	57

## EXECUTIVE SUMMARY

1. The last stock assessment for swordfish in the south eastern Pacific Ocean (EPO) was done in 2011.
2. This document presents the 2022 stock assessment. Data up to 2019 was included, which was the last year of data reported for most fleets.
3. All models were conditioned on estimated catches. The catches were computed mostly by aggregating the 5° by 5° by month catch data submitted by the CPCs into areas and quarters. Catch data missing or submitted in different formats were substituted and aggregated following a series of rules.
4. The main pieces of information, apart from the catches, are the indices of abundance. Several indices were constructed by standardizing the catch and effort data from the longline fleets of Japan, Korea, Spain, and Chile using spatiotemporal models, and from the Chilean gillnet fleet using generalized linear models. No index was considered ideal to represent the stock due to a range of limitations of each one. All indices showed similar increasing trends already apparent in the 2011 assessment.
5. The secondary pieces of information were the composition data. The most frequent size composition data available were lower-jaw-fork length. Average weight and age composition were also available, as well as eye-fork length. The composition data was weighted in the models to minimize its effect in the estimation of abundance, while allowing for accurate characterization of the selectivity of each fishery.
6. There is considerable uncertainty in stock structure. Three models were developed to represent three stock structure hypotheses. The first hypothesis (H1) assumes the stock is distributed south of 5°S and east of 150°W as in the previous assessment. In the last 10 years, catches in the equatorial region have sharply increased; the second hypothesis (H2) considers those catches as coming from the south EPO stock and extends the latitudinal stock boundary to 10°N, and maintains the longitudinal boundary at 150°W. The third hypothesis (H3) expands the longitudinal boundary to 170°W, thus including the central Pacific catches. H2 is considered as the reference case hypothesis.
7. The models were constructed using the areas-as-fleets approach. The areas were determined by maximizing the differences in sizes for each fleet among areas and minimizing it within an area using regression tree analyses. Four areas were established defined by splitting the region south of 10°N at 110°W, then splitting the resulting two areas at 20°S. The areas are consistent with the conceptual model for the stock and approximate the seasonal movement. For stock structure hypothesis H1, the same areas as the previous assessment were used (two areas split at 90°W), for comparative purposes.
8. The catch data compiled for the EPO south of 10°N showed a dramatic increase of catches since the mid-2000s. The average catch per year from 2000 to 2009 was about 15,000 tons, while the average catch per year for 2010 to 2019 almost doubled to about 29,000 tons. In the last three years of the compilation (2017 - 2019) the average catch was about 34,000 tons. The fleets that are currently the most important are the Spanish longline fleet, which catches about 30% of the total catches in weight, followed by the Chilean gillnet fleet with 22%, and the Ecuadorian longline fleet with 20%.
9. An initial reference model (Model 0) reconciled the simultaneous increase in catches and in the indices by a gradually increase in recruitment, through an increase in the estimated recruitment deviates, which are assumed to be independent and identically distributed (iid) following a normal distribution. The trend in recruitment deviates violates the iid assumption, indicating model misspecification. The same results were obtained regardless of the stock structure hypothesis.

10. Four alternative hypotheses that may explain the simultaneous increases in catch and indices of abundance were investigated, through the implementation of different models based on modifications of Model 0:
  - Model 1: Real increase in productivity. The increase in recruitment was modelled using an estimated trend so that the recruitment residuals no longer have a pattern and satisfy the assumed iid distribution.
  - Model 2: Increase in availability. Since indices derived from different fleets and gear show increase in density, the apparent increase may not be an effect of change in strategies of a particular fleet or type of gear, but rather a general change in availability to all the gears. This model is fit only to composition data.
  - Model 3: Increases both in productivity and availability. A combination of the two hypotheses above, since the underlying cause for increased availability may also be favorable to the population and may have caused the increase in productivity (higher recruitment). The model is fit to all the data, and a random walk in catchability is estimated for some indices
  - Model 4: Stock structure and connectivity. Indices derived from fleet in the western Pacific Ocean show increase in density at similar times that the indices in the EPO ([SAC-13-INF-M](#)). Connectivity between the equatorial area and the south sub-tropical EPO seems to have increased after 2010, perhaps the connectivity also increased with the Western and Central Pacific Ocean (WCPO). This model includes catches in the WCPO up to 170°W.
11. To some extent Models 2 and 3 remove the trend in recruitment, while Model 1 assumes it is a true increase in productivity through an increasing trend in average recruitment
12. The IATTC is yet to adopt reference points for S EPO swordfish. Dynamic reference points were used as an illustration to report the stock status, due to the potential changes in productivity. According to arbitrary biomass reference points simply used for comparative purposes (a limit reference point of 20% unfished biomass and target reference point of 40% unfished biomass), the stock may be approaching the biomass TRP if the increase in the indices is due to increase in both productivity and availability (Model 3). The stock would be below the biomass TRP for the other hypotheses.
13. The fishing mortality was measured as the effect in the spawner biomass per recruit with relation to the spawner biomass per recruit in the unfished condition (SPR). Large SPR are indicative of low fishing mortality, thus a proxy for fishing mortality is  $1-SPR$ . All models estimate a strong increase in fishing mortality since the start of the fishery. The fishing intensity is slightly above the fishing intensity TRP for Model 3, and below for the other model.
14. There is not enough information in the current data to determine the relative plausibility of the hypotheses. However, there is external evidence that increase in productivity of the stock maybe reasonable due to increase in the main prey of swordfish in the south EPO, the jumbo squid. If this is the case, management of the stock should account for potential decreases in productivity if the prey species decreases in abundance.
15. Future research should focus on information that could help discriminate among these hypotheses such as close kin mark recapture, tagging studies, habitat modelling and investigating changes in habitat over time, and investigating changes in fishing strategies. Models that include predator and prey dynamics may provide insights into the driving forces behind the south EPO swordfish stock apparent increase in productivity.

## 1. INTRODUCTION

This report presents the results of the benchmark stock assessment for swordfish (*Xiphias gladius*) in the south eastern Pacific Ocean (EPO), conducted using Stock Synthesis (version 3.30.19), an integrated statistical age-structured stock assessment modeling platform (Methot and Wetzel 2013, Methot et al 2020). Auxiliary plots and analysis were done using the R library *r4ss*<sup>1</sup>. This is the first assessment of the species undertaken by the IATTC's scientific staff in the last 10 years, following the workplan established in 2020. All model input files and output results for this assessment are available in [html](#) and [pdf](#) formats.

### 1.1. BACKGROUND

The Inter-American Tropical Tuna Commission (IATTC) mandate under the Antigua Convention is to ensure the long-term conservation and sustainable use of tuna, tuna-like species, and other species in the EPO, which it achieves through promoting, coordinating, and conducting scientific research, and adopting conservation and management measures. This includes swordfish, which is a target species in the EPO of both high-seas longline fisheries and coastal and recreational fisheries.

The IATTC's staff last assessed the south EPO swordfish stock in 2011 ([Hinton and Maunder 2012](#)), using an integrated stock assessment model fitted to a longline-based index of abundance and age- and length-frequency data from multiple fisheries. The species was included in the staff's research workplan (IATTC-95-08). In December 2020 the staff organized the 1st Technical Workshop on Swordfish in the South EPO ([SWO-01](#)). The objectives of the workshop included to undertake a review of the current state of knowledge of the swordfish stock in the south EPO, to construct a conceptual model of the structure and dynamics of the population and its associated fisheries and to identify data sources that could be used in the 2022 stock assessment of swordfish in the S EPO. The participants listed a series of recommendations and suggestions, most of which were used in the current assessment.

Collaborative work took place after the completion of the workshop on several aspects of the data and modelling, which will be detailed in this document. In particular, the staff was graciously granted access to confidential high-resolution data from several CPCs, which allowed the estimation of some indices of abundance. For the Japanese indices, the staff worked in collaboration with national scientists.

## 2. CONCEPTUAL MODEL AND STOCK STRUCTURE ASSUMPTIONS

The conceptual model (Figure 1) for the population of swordfish in the S EPO postulates that the population has seasonal movement ([SWO-01](#)). During the austral autumn and winter (Quarters 2 and 3), the swordfish migrates towards foraging areas in the zone of influence of the Humboldt current, closer to the coast. During the austral spring and summer (Quarters 4 and 1), the swordfish moves offshore towards warmer areas where spawning occurs. The extent of the movement is unclear, but electronic tagging off California and Australia showed that swordfish are capable of extensive migrations, returning to about the same release location (Evans et al 2014, Sepulveda et al 2020).

In the S EPO, frontal areas are found in the areas of influence of the Humboldt current, where primary productivity and prey density, such as squids and mackerel, are high. In January-February large/mature individuals move to the east to feed, CPUE also increases in the Chilean fishery at that time. In July to September, those large individuals move north. Later in the year, eddies push fish to move westward and disappear from the Chilean catches. The 24°C isotherm determines the spawning ground, but the exact extent of the spawning areas for the S EPO stock is uncertain. Spawning females were found around Easter Island and females with high gonadosomatic index, an indication of the imminence of spawning, are found in equatorial areas around 180° and 140°W. Juveniles have been found from the continent to 60 miles off Peru.

---

<sup>1</sup> <https://github.com/r4ss>

Genetic and genomic studies support population differentiation in the Pacific Ocean, but the patterns are not clearcut. Genetic connectivity in form of a  $\cap$ -shaped pattern was detected by Reeb et al. (2000) using mitochondria DNA material, with indication of connection of Australia, Chile, Central Pacific Ocean up to California/Mexico and Hawaii, and some Hawaii and California/Mexico both connected to Japan, which was different from Australia. Genomic studies (Lu et al 2016) showed that there were no differences among samples from the temperate areas of the Pacific, but there were some difference among samples of tropical areas, and that tropical and temperate areas formed two separate clusters. There is a possibility that genomic differences observed between temperate and tropical clusters may be related to sex-differentiation (Dr. Alvarado-Bremmer personal communication).

In the 2011 stock assessment, the area south of 5°S was considered as the stock boundary based on the analysis of catch rates by quarter (Hinton and Deriso 1998). The catches for the S EPO stock at that time were concentrated in the areas off Chile and Peru. In the last decade, however, the catches have increased substantially in the equatorial region. Those catches need to be accounted for in a stock assessment. During the workshop, it was recommended that the central EPO area between 5°S and 10°N be considered, either in the base case or in sensitivity models. Another area of uncertainty in the stock structure are the catches west of 150°W. Right at the vicinity of 150°W towards the west, the catches are high and seem to form a continuous area from about 130°W to about 170°W. The inclusion of this area was also considered in a sensitivity. The 2022 stock assessment has an area of overlap with the 2021 S WCPO swordfish assessment ([SC17-SA-WP-04](#)), which corresponds to the overlap jurisdiction between the IATTC and the WCPFC (150°W to 130°S and south of 4°S).

Following the uncertainty in stock structure, **three hypotheses for stock structure were considered in this assessment:**

**H1:** The stock is distributed **south of 5°S and east of 150°W**, as it was assumed in the previous assessment.

**H2:** The stock is distributed **south of 10°N and east of 150°W**. This hypothesis is considered as the reference case.

**H3:** The stock is distributed **south of 10°N and east of 170°W**.

### 3. DATA

#### 3.1. CATCHES

##### 3.1.1. CATCH ESTIMATION

The catches for non-purse-seine gears are reported annually to the IATTC by individual Members and Cooperating non-Members (CPCs), pursuant to Resolution C-03-05 on data provision. Catches are reported by species, but the availability and format of the data vary among fleets. Most of the catches are taken by longline fleets. Gillnets are important off Chile. Harpoons were common until the 1980's.

The main longline fleets report catch and effort aggregated in 5° latitude by 5° longitude by month resolution, as well as aggregated for the whole EPO. IATTC databases include data on the spatial and temporal distributions of longline catches of swordfish in the EPO, at least for one year, for the fleets of distant-water CPCs (Belize, China, Chinese Taipei, French Polynesia, Japan, Korea, Spain, Vanuatu) and coastal CPCs (Panama, Mexico, and the United States). Other fleets, such as those from the coastal countries, report longline, and gillnet catches only aggregated by year for the whole EPO and assumptions about the location and timing of the catches are needed to be used to partition the catches in the spatial and temporal scales of the assessment model. The catches may be reported in weight, numbers, or both. For the current assessment, a special submission of catches by gillnet and longline by quarter for 2000 to 2019 were reported by Chile, and a special submission of trip-by-trip data on catches was reported by Ecuador for years 2016 to 2020. For Central and South American CPCs, the data available in the FAO Regional

Capture Production dataset, updated to 2019, was also consulted, through the “Regional workspace” in the software FishStatJ<sup>2</sup>, and compared to the data submitted to the IATTC, when discrepancies were found, the largest values were used, following a precautionary approach.

Updated and new catch data (up to 2019) for the longline fisheries, available to the IATTC staff as of March 9<sup>th</sup>, 2022, were incorporated into the current assessment. For years when catch may not be available, catches were set equal, by CPC, to the last year for which catch data were available. For fleets that reported catch aggregated by year and space, the data was disaggregated using the proportion of catches by quarter and area for the closest year for which data on that resolution were available. The catches of a coastal CPC that reported aggregated catches were added to the area which contained that CPC’s Exclusive Economic Zone (EEZ). For Central American CPCs and for Colombia, the catches were split by quarter using the proportion of catches by quarter from Ecuador. For years before 2000, the catches for Chile were apportioned by quarter using the proportions for years after 2000. No catches for Chile for harpoon were reported for 1987 to 1999. Since there were catches before 1987 and after 1999, absence of reporting was assumed rather than no catches, so the catches were assumed to be equal to those from 1986. All decisions on data substitution and splitting are detailed Appendix 1.

### 3.1.2. CATCH TRENDS

The south EPO swordfish stock has been exploited since the 1940’s, initially by two coastal countries, Chile and Perú. The oldest fishery is the Chilean harpoon fishery, with catches reported since 1945 (Table 1, Figure 2). Perú started reporting catches of longline fisheries soon after, in 1950. In 1954, the longline Japanese fleet started operations in the EPO, Chinese Taipei followed ten years later and Korea twenty years later. Before 1986, the stock was exploited by those two coastal fleets and three distant water fleets. The known catches in that period averaged about 3,000 t and ranged from about 650 t to about 7,800 t, with a noteworthy peak in 1950 when Perú started reporting and recorded about 7,000t. Other fleets started operations in the 1990’s, with the Spanish fleet rapidly dominating the catches.

Unlike the other distant water fleets that catch swordfish as part of their longline fishing for tunas, the Spanish fleet targets swordfish, and brought their experience fishing for swordfish in other oceans to the Pacific Ocean. The Spanish fleet has been the main player in the fishery since the early 2000’s and currently (2017-2019) accounts for 30% of the catches, while the other distant water fleets combined account for 24%.

In the late 1980’s, Chile started a longline fishery that had its peak catches in 1991 and slowly dwindled until complete cessation of operations in 2019. Simultaneously, a gillnet fishery was developed, and had an initial zenith in 1989, a decrease in the 1990’s, when Chilean longline catches were higher, rebounding again in the early 2000’s and flourishing in the 2010’s. The highest catches of the Chilean gillnet fishery were recorded in 2019.

Ecuador started reporting catches of swordfish in the 1990’s, in the order of 300 to 550 t a year until 2007, with some years of no reporting. After 2008 a thorough system of data collection was implemented. The reported catches increase above 1,000 t for most years and above about 3,000 t after 2016, mostly taken by the longline fleet, which has an oceanic-artisanal component of mother-ship boats (*nodrizas*) with associated fiber-glass skiffs (*fibras*) (Martínez-Ortiz et al 2015). The all-time high catches of swordfish were in 2019. Gillnets are also used, mainly in areas closer to the coast, but the catches from this gear before 2016 are unknown. For 2016 to 2020, data from the special submission by Ecuador allowed for the estimation of gillnet catches, which are of the order of hundreds of tons.

Similar to Chile, Perú has also switched to gillnets and, since the late 2000’s, it was estimated that gillnets

---

<sup>2</sup> Available from <https://www.fao.org/fishery/en/topic/18238?lang=en> (accessed on 03/09/2022)



were the most commonly used gear (Guevara-Carrasco & Bertrand, 2017). In recent years, the peak of the catches was in 2012 with about 3,000 t, much lower than the all-time record of the 1950's.

Costa Rica is the next coastal country in order of importance for the swordfish fishery. The catches are taken by longlines. The reported values have ranged between 20 and 2,200 t, since 1991, with average of about 600 t.

Other coastal countries that have reported catches of swordfish allocated to the areas south of 10°N are Colombia, Guatemala, Honduras, Nicaragua, and Panamá, with the largest catches being reported by Panamá in 2019 (1300 t).

The fisheries from the coastal countries account for 46% of the recent catches (2017-2019), of which the Chilean gillnet fishery is the most important (22%) followed by the Ecuadorian longline fishery (16%).

In the mid 1990's several fleets started operations in the EPO, and the catches increased to about 12,000 t in 1992. In that decade, the catches were always above 4,500 t and average about 8,000 t a year. In the 2000's the catches again increased, never dropping below 8,000 t a year, averaging about 15,000 t. In that decade, the highest catches were in 2002, with the record of about 22,000 t. In these two decades, a decline was observed after each peak. In the 2010's, there was yet another substantial increase in the catches that ranged from about 21,000 t to the highest historical level of 36,500 t in 2018. **In the last decade the catches have averaged about 29,000 t a year, almost the doubling in relation to the previous decade.** In the last two years considered in this assessment, the catches have reached their all-time high in 2018 36,500t and showed a sign of a slight decline in 2019 to 34,600t.

### 3.1.3. FISHERY DEFINITIONS

This assessment, as the previous one, uses the "areas-as-fleets" approach, where spatial information is considered indirectly by dividing the assumed geographical distribution of the stock into smaller areas with different availability of ages/sizes/sexes of fish (Cope and Punt 2011 Waterhouse et al. 2014). The availability, as well as the contact selectivity of the gear, are then summarized in one selectivity function. Thus, the catches were aggregated in "fisheries" defined by the spatial area of operation, gear, origin of the fleet, and unit of reporting<sup>3</sup>, to hopefully combine similar fishing strategies and regions with similar availability so the effect of catches in different components of the population are accurately represented in the assessment model. **By combining spatial information, origin, and gear, and unit of reporting 11 fisheries were defined for H1 and 21 fisheries were defined for H2/H3 (Table 2).**

The fishery definitions vary by stock structure hypothesis. For hypothesis H1 the same fisheries definitions used in the 2011 assessment ([Hinton and Maunder 2012](#)) were maintained, so that direct comparison with that assessment can be done. The two areas defined in the 2011 assessment were coastal (east of 90°W) and oceanic (90°W to 150°W). For the H2 and H3 hypotheses the areas were determined by splitting the length frequency data available using regression trees (Lennert-Cody et al 2013). The analysis also included quarters and cyclic combinations of quarters as splitting variables, because the availability of swordfish may depend on the seasons for some regions of the EPO. When compared to the spatial variables, season, however, did not explain enough variability to be used to define fisheries. Four areas were defined for H2, as the four quadrants obtained by splitting the region at 100°W and 20°S. For H3, the catches of two additional areas in the central Pacific (150°W to 170°W, split at 20°S) were added to the adjacent areas in the EPO, simply as the continuation of the neighboring EPO areas.

Spatial information of the catches is available for the distant water fleets, but it is lacking for the coastal

---

<sup>3</sup> in numbers and in weight, weight used to convert between numbers and weight is calculated internally in the assessment model

CPCs' fleets, which in general operate closer to the coast. For H1, the catches for Chile and Perú were allocated to the coastal area (area 3), and the catches for the rest of the coastal countries were not included. For H2 and H3, the Chilean longline catches were allocated to the southern coastal area (area 5, south of 20°S) and the gillnet to the northern coastal area (area 4, south of 10°N and north of 10°S), while the Peruvian catches, as well as the catches for the rest of the coastal countries were allocated to the northern coastal area.

Fleet origin was also included in the definition of fisheries. Three origins were defined as: coastal, which includes all coastal countries that fish using smaller boats; distant water, which includes all industrial longline fleets of non-coastal CPC except Spain, which was separated in another group. Spain is the only distant water fleet to target swordfish, the other fleets may have swordfish as secondary target, and bigeye tuna as primary target. The fishing strategies used by these two groups may differ. Spain is the fleet with the most widespread distribution, while the other distant water fleets are mostly concentrated in the equatorial areas towards the central Pacific Ocean, with exception of Japan that can fish also in the coastal areas (area 4 in H1 or areas 4 and 5 in H2/H3).

Catches in all areas have increased in the last decades (Figure 3), **with the largest increase being in the northern coastal area** (area 4 in H2/H3, Figure 4), **where the catches are about three times what they were in the previous decade**. The catches also show different seasonality according to the areas. Most of the catches are taken in quarters 2 and 3 in the coastal areas (area 4 in H1 and areas 4 and 5 in H2/H3, Figure 5). In contrast, most of the catches are taken in quarter 4, and to some extent in quarter 1, in the offshore areas. This seasonality is consistent with the conceptual model for the stock.

### 3.2. INDICES OF ABUNDANCE

In Stock Synthesis, a 'survey' is a representation for data that does not have associated catches, such as indices of abundance and their corresponding age/length compositions. Six surveys were defined for H1 and nine surveys were defined for H2/H3 (Table 2), coming from the indices of abundance described below.

An ideal index of abundance would represent the population well and would be proportional to the population size. Ideally, an index should encompass periods of contrasting exploitation rates to be informative, thus an index that starts when the exploitation rate was low (at the beginning of the exploitation history) is preferable. For swordfish stocks, as for most large pelagic stocks, no fisheries independent surveys are available, and indices of abundance are constructed based on catch and effort information (and most recently on size or age structure of the catches, Maunder et al. 2020). Candidate data sets for the standardization need to be scrutinized to assess whether the assumption of representativeness is likely to be met. Ideally, an index should encompass periods of contrasting exploitation rates to be informative, thus an index that starts when the exploitation rate was low (at the beginning of the exploitation history) is preferable.

For south EPO swordfish, four candidate data sets were analyzed to produce indices of abundance (Figure 6). None can be considered ideal, and their limitations and advantages are discussed in Table 3. Of all indices constructed, the indices from Japan ([SAC-13-INF-N](#)), Chile and Spain were included in the models for H2 and H3. For H1, similarly to the 2011 assessment, indices were constructed for the coastal and the oceanic areas (Figure 7) based solely on the standardized CPUE from the Japanese fleet ([SAC-13-INF-N](#)). This was done by summarizing for each area (offshore and coastal) the spatial predictions for density derived from the Japanese indices. Additionally, a gillnet index from Barraza et al. (unpublished) and another from Korean longline data ([SAC-13-INF-M](#)) were also available, but not used to fit the model. All indices show the sharp increase in the early to mid-2000's, mainly in the coastal areas.



### 3.3. COMPOSITION DATA

Length, age, or weight compositions are available for most fleets.

For distant water longline fleets all available length composition data were used. Most of the data come from the Japanese fleet, which reports eye-to-fork length (ETF). That measure was transformed to lower-jaw-fork-length (LJFL) (Table 4). The temporal resolution was month and the spatial resolution varied (e.g. 1° by 1°, 5° by 5°, 5° by 10°). The data was aggregated by fishery and by quarter.

For Chile, the *Instituto de Fomento Pesquero* (IFOP) made age and size composition data available to the staff. LJFL data was available for 2000 to 2019 for gillnet and longline fisheries in a 2° by 2° by month resolution. Details on the data collection and ageing methodology can be found in Barría Martínez et al (2021) and Cerna (2009).

For Ecuador, the Undersecretariat of Fisheries Resources of Ecuador made size composition data available to the staff. LJFL data was available for 2016 to 2020. The data for 2016-2017 showed a distribution centered on very low sizes, while the data for 2018-2020 showed distribution centered in larger sizes like those from the Chilean fleet to the south. The composition data for Ecuador was not used to fit the model because the strong shift in size is not understood. The data was left in the model to see whether the model was able to predict it.

In stock-structure hypotheses H2/H3 the selectivities for the coastal fisheries were mirrored to each other, because only sufficient data for one area was available.

The length compositions for the catches were aggregated in 10-cm intervals from 50 cm to 310+cm. The input sample sizes were computed as the total number of fish sampled divided by 100. For the Spanish fleet the data seems to have been raised to the catch before submission to the IATTC and there was no information on the original sample sizes, as the number of fish in the length frequency data base is similar to the numbers of fish in the catch database, but the spatial coverage is different. The length compositions for the indices of abundance were aggregated in 10-cm intervals from  $\leq 50$  cm to  $\geq 270$  cm (Spanish indices) or 20-cm intervals from  $\leq 80$  cm to  $\geq 300$  cm (Chilean index). For the Japanese fleet, standardized average weight was also obtained ([SAC-13-INF-N](#)).

### 3.4. DATA WEIGHTING

The objective function includes data likelihoods and parameter penalties. The likelihood for each data component includes a weighting factor related to the variability of each data point and an overall weighting ( $\lambda$  or variance) for the component (Table 5). Likelihood functions encompass not only the sampling (observation) variability, but also model misspecification and unmodelled process variability. To accommodate those sources of variability, indices that were chosen to best represent each period were given fixed CV to be either 0.2 (I3\_JPN\_early, I5\_JPN\_late) or the variability estimated from the spatio-temporal model used to produce the index added to a constant of 0.1 (I1\_Chile\_Q2, I2\_Chile\_Q3) so that on average the CV would be about 0.2. The other indices had the CV set equal to either 0.2 (I4\_JPN\_mid) or to the estimates from the spatiotemporal models plus an extra variability parameter to be estimated within the assessment model. The composition data was weighted using the Francis approach that accounts for correlations in the residuals, which gives more weight to the indices while weighting the composition data enough to be able to estimate the selectivities. The only exception to that was the weighting for the composition data assumed to represent the stock. The standardized length composition associated

with the Spanish and Chilean indices of abundance, were assumed to have a sample size of 50 for each year and quarter. The standardized average weight associated with the Japanese indices of abundance (I4\_JPN\_mid, I5\_JPN\_late) was set equal to the estimated variability in average weight (computed as the variation on the average weight predicted by the spatiotemporal model for each 1° by 1° cell).

## 4. REFERENCE MODELS

### 4.1. GENERAL MODEL STRUCTURE

An initial reference model (Model 0) using the stock structure hypothesis 2 (10°N to the south and 150°W to the east) was set up, which was modified to produce the sensitivity models (Table 4) and the models corresponding to the alternative hypotheses explaining the simultaneous increase in catches and indices. Several assumptions for the model structure are the same as in the previous assessment and are shared among models as summarized in Table 4. The individual growth curve and the length-weight relationship are defined by sex (Figure 8). The natural mortality is the same for both sexes and equal to 0.4. Diagnostic analyses such as age-structure production model (ASPM) and catch-curve analysis (CCA) were also computed for Model 0 (Carvalho et al 2021, Minte-Vera et al 2021)

### 4.2. SELECTIVITIES

Selectivities were estimated using double-normal distribution functions, which allowed estimation of domed or asymptotic selectivities, and splines or logistic functions (Table 6). For some fleets it was necessary to use splines to allow for more flexibility in the shape of the function. Splines and initial values for all selectivities were set up using the *empirical\_selectivity* R library (Olivero-Ramos 2021, available from GitHub<sup>4</sup>)

Time blocks for selectivity were included for some fisheries. The Spanish fisheries operating in the coastal areas (F8 and F9) had a block from 2000 to 2019. Around the year 2000 the gear used in these fisheries underwent a complete change in configuration and operation, when it was changed from the traditional method to the “American longline” (Mejuto and García-Cortés 2005). Therefore, the Spanish coastal fishery was modeled with a time-block separating the fisheries into pre- and post-2000. Examination of residuals in the size-frequency data from preliminary analyses clearly indicated a change in selectivity, indicating the need for this additional structure in the model. The distant water fleets operating in the coastal area (F12) also had a block from 1994-2019, when the fleet changed the materials of the lines and hooks-between-floats ([SAC-13-INF-M](#)).

### 4.3. MODELS BY HYPOTHESIS

Model 0 reconciles the increase in catches with the increase in the indices by estimating a steady trend of increased recruitment though a trend in the estimated recruitment deviates. This apparent increase in recruitment could be due to model misspecification. There are other hypotheses that may explain the observed pattern: 1) increase in productivity, 2) increase in availability, 3) increase in both productivity and availability, and 4) increase in connectivity with the WCPO. These hypotheses were investigated further by implementing several models, of which four were selected (Table 7) to best represent them as describe below:

---

<sup>4</sup> `remotes::install_github("roliveros-ramos/fks")`  
`remotes::install_github("roliveros-ramos/empirical.selectivity")`

**Model 1: Increase in productivity.** In this hypothesis the possibility that the productivity of the stock has increased gradually from a low productivity phase to a high productivity phase, due to changes on the average recruitment. In Model 0, the recruitment deviates model how the recruitment differs from the average recruitment in each year and are penalized assuming an iid log-normal distribution. A trend in the estimated recruitment deviates violates this assumption. To better represent the increase in recruitment hypothesis and avoid the recruitment deviate iid assumption being violated, Model 1 implements a trend in the regime parameter for recruitment. The trend starts at 0, in 1945, when the (logarithm of) virgin recruitment ( $\ln R_0$ ) is fixed to be equal to a baseline. The baseline  $\ln R_0$  was obtained from an ASPM for an early model (years 1945 to by 1993). The model estimates a logistic curve to represent the trend, the estimated parameters are the width of the trend, the mid-year of the trend and the final regime value. The lower and upper limits for the mid-year of the trend were specified as 1995 to 2019.. Model 1 also estimates recruitment deviations to allow for variation in recruitment around the trend.

**Model 2: Increase in availability:** This hypothesis explores the possibility that the increase seen in all indices of abundance is in fact an increase in availability of the fish to all the fleets and gears, maybe due to a common cause such as a change in the environment. This implies that the indices are not a proxy for population abundance. Thus, this model is implemented by fitting a model like Model 0 only to catch, mean weight, age, length, and generalized size composition data (like a catch curve analysis, Carvalho et al 2021). The change in availability to the indices is computed as the difference from the expected values for the indices given Model 2 and the observed indices. The relationship between the catchability coefficients by year and the vulnerable biomass are compared to assess whether they follow the same trend among indices.

**Model 3: Increase in availability and increase in average productivity:** This hypothesis is implemented using a model like Model 0 but estimating time-varying catchability for all indices that include the “transition period” when the availability may have increased (that is from about 1995 to about 2009). The indices are assumed to vary over time following a normal distribution with mean zero standard deviation of 0.3, which is approximately equal to the assumed observation error, and autocorrelation of 0.4, estimating a  $\ln R_0$  and recruitment deviations. If the productivity increased, the estimated  $\ln R_0$  will be larger than the baseline  $\ln R_0$  estimated by the ASPM for an early model (years 1945 to by 1993). Initially this hypothesis was done by including a regime shift trend as in M1, however the model did not converge. Therefore, this simplified model was formulated.

**Model 4: Connectivity and stock structure:** The ideal model to represent this hypothesis is a spatial model that allows for movement from the WCPO to the EPO, and would include tagging data or at least movement rate estimates based on tagging data (e.g. Patterson et al 2021). With the current data, the model implemented to represent this hypothesis is simply like Model 0 but also includes the catches in the WCPO south of 10°N between 150°W and 170°W.

## 5. RESULTS

### 5.1. INITIAL REFERENCE MODEL (MODEL 0)

Model 0 had a small maximum gradient at the solution and produced an inverted Hessian matrix indicative of convergency. The model was able to, on average, fit the size composition data well, indicating that the catches should be taken at about the correct sizes and ages from the population and that there is a good presentation of the sizes included in the indices of abundance (Figure 9). The only data that is not predicted well are the length frequencies for F4\_LL\_Coast\_A4, which are not fit to the model and correspond to data from Ecuador that have a mixture of years with small length frequencies followed by years with larger length frequencies. The estimated selectivities indicated that, apart from F3\_GN\_A5 that was

assumed to have asymptotic selectivity, the fisheries F7\_ESP\_A3 and F5\_LL\_Coast\_A5 caught large fish (Figure 10). The selectivity of the Spanish fleet operating in the coastal areas (F8\_ESP\_A4), switch in year 2000 from a narrow range of selectivity centered mostly between 150 to 200 cm, to wider range, catching fish from 100 cm to the maximum size (350 cm). The distant water fleets (F12\_LL\_DW\_A4) had the opposite change around year 2000, going from a wide range of sizes having high selectivity (*i.e.* from 100 cm on), to a narrow range centered mostly on juveniles of about 80 to 100 cm. For the indices, the selectivity chosen to be asymptotic was I3\_JPN\_early. The selectivity for I6\_ESP\_Q1, however, was estimated to be almost asymptotic, and the selectivity for I9\_ESP\_Q4 catches large fish.

Model 0 had a good fit to the indices of abundance because the increasing trend in the indices was matched with a continuous increase in recruitment estimated since the mid-2000 (Figure 11). An ASPM based on Model 0 was unable to track the indices (Figure 11) indicating that the catch was not consistent with the index of abundance and can only be explained by an increasing trend in recruitment. A CCA based on Model 0 was unable to predict the indices, indicating that the trend implied by the composition data is in contradiction with the indices (Figure 11).

Changing the model to an update of the 2011 assessment, which considers the H1 hypothesis for stock structure (northern boundary at 5°S), did not resolve the recruitment increasing trend (Figure 12). In fact, the 2011 assessment already had the same recruitment pattern starting in 1990.

Sensitivity models showed the same steady increase in recruitment (Figure 13). The pattern in the recruitment deviations does not get resolved when the natural mortality is assumed to be 0.2 instead of 0.4, or the steepness is assumed to be 0.75 instead of 1, as expected. These assumptions reduce the productivity of the stock, which must compensate with even larger recruitments to be able to account for the recent catches. Estimating the natural mortality rate ( $\hat{M} = 0.269$ ) did not resolve the recruitment pattern either.

## 5.2. MODELS BY HYPOTHESIS

The models implemented to represent the four hypotheses that may explain the increase in the indices with simultaneous increase in the catches converged as indicated by the estimation of the Hessian matrix, the corresponding variance-covariance matrix, and a low gradient at the MLE solution. Model 4 presents the same recruitment trend pattern as Model 0, as expected, since the only difference between those two models is the increase in catches given by the inclusion of the central Pacific Ocean catches (Figure 14). Models 1 and 2 show a random distribution around the mean recruitment in the later years, but Model 1 does it by modeling a trend in average recruitment. Model 3 decreases the recruitment pattern, but does not completely resolve it, since the increase in productivity is not modelled explicitly using a trend as in Model 1.

The estimates of recruitment are very uncertain for the period before mid-1970's (Figure 14). For all models, there is a declining trend in recruitment from mid-1970'd to mid-1980's. The same pattern is repeated twice in the next 20 years. After year 2000 the estimates of recruitment vary by hypothesis, but cycles are apparent in all hypotheses (Figure 14).

The highest estimate of current spawning biomass is for Model 4, as expected since this model considers the stock to be larger (Figure 15). After 1970's, the uncertainty in the estimates, however, overlaps with those for Model 0 and Model 1. The uncertainty for the spawning biomass may be underestimated for Model 1 and Model 2, because  $\ln R_0$  is set to a fixed value equal to the estimate of an early model (see 4.3. Models by hypothesis). Model 3 estimates a stable spawning biomass in the last 20 years, due to

increase in estimated productivity (higher  $\ln R_0$ ), apart from increased availability. Model 2 shows a much larger and uncertain estimate of virgin biomass. It shares the decline in the late 1970's and early 1980's, and to some extent the period of stability of the late 1980's and 1990's, with the other models, but shows a continuous decline in the spawning biomass starting in the early 2000's because fishing occurs on a population assumed to have no trend in productivity. To be able to support the current catches without an increase in productivity, Model 2 estimates a much larger overall productivity.

All models estimate about the same depletion up until year 2000, when the differences among models start to be noticeable, since each model explains the increase in the indices and catches in a different way (Figure 16). All models estimate almost no depletion until the early 1970's, then a decline in spawning biomass from the mid-1970's to the late 1980's, thus an increase in depletion, followed by a period of low biomass that lasted about 10 years. That period was followed by a period of increase in spawning biomass from late 1990's to early 2000's. Models 1, 2 and 3 have markedly different spawning biomass trajectories after the early 2000's. The increase in productivity model (Model 1) estimates that the population from 2010 on is even larger than the virgin conditions. Since Model 1 estimates an increase in productivity, the spawning biomass tends to increase steadily after 1999 until it levels off at a second productivity regime after 2012. Model 2 estimates a decline that results in a depletion of about 50% in the later years, since it is hypothesized that the increase in catches is a result simply of increase in the availability of swordfish to all fishing gears. Model 3 follows a pattern intermediate between Model 1 and Model 2, because not only the overall productivity is estimated to be larger, but also the model estimates recruitment trends since the year 2000 to be able to fit better the indices of abundance.

The differences among models are marked after year 2000 when the catches increase substantially and more composition data are available. The indices of abundance are not useful in discriminating among hypotheses, since the estimation of variable catchability, would certainly fit the indices better (Appendix 3). Thus, it is key to scrutinize the fits to the composition data and average weight data to investigate whether these data support one hypothesis more than the others. Table 8 shows the NLL difference between the model that fits a particular data component the best, and the analyzed model. Only those data components with more than 3 NLL units were analyzed. The length composition data are fit better by Model 2 in general, indicating supports to the increase in availability hypothesis. The increase in productivity and availability hypothesis is supported by several data components related to the longline fleets operating in the coastal areas (e.g. generalized size comps associated with the Chilean longline indices I1\_Chile\_Q2, I2\_Chile\_Q3, and the length and age composition for fishery F5\_LL\_Coast\_A5, length composition for F8\_ESP\_A4)

### **5.3. STOCK STATUS**

The IATTC has yet to establish reference points for swordfish in the S EPO. The status of the swordfish stock in the northeast Pacific Ocean has been, as in the past, presented in terms of management parameters based on MSY. Since the main goal of the Antigua Convention is to "... ensure the long-term conservation and sustainable use of the fish stocks covered by [the] Convention, in accordance with the relevant rules of international law," and calls on the Members of the Commission to "... determine whether, according to the best scientific information available, a specific fish stock ... is fully fished or overfished and, on this basis, whether an increase in fishing capacity and/or the level of fishing effort would threaten the conservation of that stock", in this assessment we interpret the general guidance given by the Antigua Convention to be the need for determination of whether the stock is able to replenish itself given the

current fishing mortality. Also, because there is large uncertainty in what the productivity of the stock is, reference points based on MSY seem inadequate. Thus, we will focus the stock status determination on potential limit reference points.

Due to the possibility of large changes in the productivity of the stock, it is advised that dynamic reference points be used, as they take the variability in productivity into account when computing reference levels. For completeness, two types of candidate limit reference points are shown, equilibrium and dynamic ones. The equilibrium limit reference points (LRP) are based on what is used for or tropical tunas in the IATTC ([Res C-16-02](#)). The IATTC adopted a biomass limit reference point equal to the spawning biomass corresponding to a reduction of 50% recruitment when the steepness of the Beverton-Holt stock recruitment curve is assumed to be 0.75. This corresponds to a depletion of about 7.7%. The fishing mortality reference point is the fishing mortality that brings the population to that depletion level, given the current mix of selectivities in the fisheries. The target reference point (TRP) is the level corresponding to the MSY. It was interpreted as a dynamic value in the latest tropical tuna stock assessments (Minte-Vera et al 2020, Xu et al 2020) but as an equilibrium level previously (Minte-Vera et al 2018). The equilibrium MSY level for YFT was about 27% of SSB<sub>0</sub>, while for BET was 23% of SSB<sub>0</sub>. For swordfish it should be higher since it is a longer-lived species than tropical tunas with low natural mortality. The dynamic reference points are based on the WCPFC ones. The WCPFC adopted a dynamic biomass limit reference point for all stocks under their jurisdiction of 20% of the unfished biomass (20%SSB<sub>F=0</sub> when time t is equal current time) (<https://www.wcpfc.int/harvest-strategy>). The unfished biomass is defined as what the current biomass would be without fishing, thus considers the estimated variability in recruitment. For target reference points, two values are computed 40% SSB<sub>F=0(t)</sub> and 50% SSB<sub>F=0(t)</sub>, which are values assumed in the MSE for NP albacore ([NC17-IP-06](#)), which is longer lived than tropical tunas, and are shown here for reference only. Again, the values presented are for the sole purpose of comparing among models, as reference points for swordfish are yet to be chosen by the IATTC.

Based on the equilibrium RP, all models are above the LRP for tropical tunas (Figure 16). Based on the dynamic RP, all models are above the LRP of 20% unfished biomass (Figure 17). The stock is approaching the TRP of 40% unfished biomass if the increase in the indices is due to both an increase in productivity and an increase in availability (Model 3). If the increase in the indices is indeed a real increase in productivity, the stock is above 50% of the unfished biomass even if H1 or H3 are considered as hypotheses for stock structure (Models 1, 4 and H1). Although some data components support one hypothesis over the others, it is deemed that there is no clear-cut information in the current data to determine the relative plausibility of the hypotheses.

The fishing mortality is measured as the decline in the proportion of the spawning biomass produced by each recruit due to fishing in relative to biomass per recruit in the unfished condition (SPR) (Goodyear 1993). Large SPR are indicative of low fishing mortality, thus a proxy for fishing mortality is 1-SPR. For example, to maintain the population at a dynamic biomass target reference point of 40% of SSB<sub>F=0(t)</sub>, the fishing intensity would be 0.6 on the long run.

All models estimate a steady increase in fishing intensity from the 1970's until the year 2000, when catches increase (Figure 18). After 2000, model 3 showed a steeper increase in fishing intensity than the other models and estimates the highest current fishing intensity followed by Model 2, increase in availability. Those two model estimates that TRP of F50% has been breached.



The phase plots indicate that the LRP has not been breached in any of the four hypotheses plus the hypothesis H1 of smaller stock. (Figure 19). The sensitivity models, however, indicated that if the natural mortality is lower, both the biomass and the fishing intensity LRP would have been breached.

The impact of fishing is the highest for the Model 3 – productivity and availability, followed by Model 2 – availability because Model 2 estimates a much larger overall productivity to account for the current high catches (Figure 20).

## 6. DISCUSSION

The simultaneous increase in the abundance indices and in the catches of the S EPO swordfish stock led to the development of four alternative hypotheses to explain those patterns. The first hypothesis is that there is a real increase in productivity in the south EPO swordfish stock, and the indices are tracking a true increase in the population abundance. The second hypothesis is that there are changes in availability in the stock, which can be translated into changes in the catchability parameters over time for each index, making the indices not proportional to abundance. The third hypothesis assumes there are both changes in production and changes in availability. Finally, the fourth hypothesis is that part of the western and central south Pacific catches are in fact from the EPO, thus part of the productivity there moves to the EPO. This was the simplest way to model connectivity with the WCPO with the available data, which is effectively assuming that the connectivity is always high, as in a larger stock.

Are there conditions in the South Pacific that can potentially cause either an increase in the productivity of the stock, an increase in the availability to the fisheries, or both? Is the possibility of an increase in the connectivity with the western and central south Pacific?

To scrutinize the hypothesis of changes in productivity, a review of the origin of the productivity for the S EPO swordfish stock is needed, and of factors that may influence its variability. The S EPO swordfish stock is highly associated with the Humboldt current system (HCS), one of the most productive marine ecosystems in the world (Thiel et al 2007). The HCS is the eastern portion of the basin-scale southeast Pacific anti-cyclonic gyre, limited by the West Wind Drift (WWD) in the south and the equatorial current system in the north. The HCS is characterized by a northward flow of cold surface water originated at subantarctic latitudes and a strong upwelling of cool waters originated in the equatorial areas. The nutrient-rich waters sustain a large primary production, which is the basis for abundant production in higher trophic levels. The HCS extends from latitude 42°S, in south Chile, up to Ecuador and the Galapagos Islands, in the equator. The upwelling occurs in the northern portion almost permanently and in the southern portion in a seasonal way, with localized high upwelling areas (*e.g.* main upwelling centers are 20-22°S, 32-34°S and 36-38°S). The northern latitude at which the WWD approaches the continent shifts seasonally from 35°S to 40°S in austral winter to ~45°S in austral summer. The subsurface waters of the HCS have low oxygen. The HCS presents intense seasonality given by the periodic intrusion of equatorial waters due to the alternations of the season. The areas with the highest catches of swordfish in the S EPO are in the main upwelling areas of the HCS. Off the coast of Chile, swordfish move seasonally from 40°S starting in March each year to about 18°S by February in the next year, roughly following the spatiotemporal displacement of the 18° and 17°C isotherms (Espindola et al 2011).

The seasonality of the HCS interacts with the El Niño Southern Oscillation (ENSO). Oceanic ENSO signals originate in the Western Pacific and move eastward as equatorial Kelvin waves that propagate poleward up to 40°S as coastally trapped waves (CTWs) (Thiel et al 2007). The ENSO incurs strong interannual variability on the mean seasonal pattern, with decreasing intensity as one moves south. During the warm El Niño phase, the sea level height raises, the thermocline deepens, and the sea surface temperature anomaly becomes positive in the eastern EPO. The Peru coastal current (PCC) and the Chile Coastal current

(CCC), that normally flow towards the equator, may decrease in intensity or even reverse flow. The CTWs have high energy. The upwelling may be of warm nutrient-poor water from above the deepened thermocline. During the cold La Niña phase, the coastal sea level decreases, the thermoclines shallows, and the sea surface temperature anomaly becomes negative. The coastal equatorward flow of PCC and the CCC strengthens. The CTWs weakens.

Swordfish is one of the key species in the pelagic food web in the central and eastern PO (Lin and Zhu, 2020). They prey mostly during the day, can be either basking in surface waters, preying in the mixed-layer distribution between sub-surface waters and the thermocline, or doing prolonged dives below the thermocline, often to depths of > 600 m (Moore 2020, Sepulveda et al., 2010; Evans et al., 2014; Sepulveda et al., 2018). During the day, swordfish are actively preying in the oxygen minimum layer and during the evening they prefer the shallow waters.

### 6.1. INCREASE IN PRODUCTIVITY

Swordfish are one of the main top predators of the HCS (Trophic level 5.2, [SAC-13-10](#)). In recent years their preferred prey, Jumbo squid (*Dosidicus gigas*, Ibanez et al 2004, Zambrano-Zambrano et al 2019), has increased in abundance, which may justify an increase in productivity of the swordfish stock. Catches of squids have increased in a disproportional way in the southeast Pacific Ocean in comparison with neighbor areas in the south Pacific (Figure 21). The catches increased fifteen-fold from the early 1990's to the early 2010's in the Southeast PO, fourfold in the western central PO, doubled in the eastern central PO, and have declined 30% in the southwest PO. Although some of the increase in catches may be consequence of the increase in effort, it seems that the S EPO has become an important hotspot for squid, especially jumbo squid. Prior to 1989 the landings of jumbo squid in Peru were less than 1000 t a year. Directed fishing started only after 1991 and in 1994 the catches were close to 200,000 t (Csirke et al 2015). The higher abundance of this species in the EPO has attracted a large fleet of squid-jiggers, catching more than half a million tons of Jumbo squid a year, making it the third largest fisheries resource in biomass in the HCS, after the anchovy and the jack mackerel (Montecino and Lange 2009). The range expansion of jumbo squid was also observed in the northern hemisphere (Zeidberg and Robison 2007).

Jumbo squids are fast growing, short-lived animals, with plastic life-history and fast response to environmental changes. Their population is usually composed of individuals from a single year-class (Csirke et al 2015). However, in La Nina conditions, the squids may increase survival to 1.5-2 years, as well more than double in size than in an El Niño year, associated with low temperatures during a key developmental period (Arkhipkin et al 2015). The sudden increase in biomass in the jumbo flying squid in the La Niña years of 2000-2001 maybe related both the increase in somatic growth and in longevity.

The conditions for expansion of the jumbo squid may be persisting after the 2000-2001 La Niña Years. After the year 2000 and at least up to 2012, the jumbo squids fished off Peru were almost three times larger than those caught in from 1989 to 1999 in sizes, and the areas with high CPUE have expanded considerably (Csirke et al 2015). Acoustic estimates of jumbo squid population abundance inside the Peruvian EEZ indicated an increase in abundance in from less than 200,000 t in 1999 to 1.8 million t in 2004 (Csirke, 2015). In 2015, the acoustic estimates were about 0.8 million t just in the Peruvian EEZ. Off Chile, the biomass of jumbo squid increased about 17x from about 40,000 t in 2001 to about 680,000t in 2003 (Alarcón-Muñoz et al 2008). In 2012, the jumbo squid was the main species caught by the artisanal fisheries in Perú (Guevara-Carrasco and Bertrand, 2017). This increase in the population of the main prey species of swordfish may have created the conditions for the increase in productivity of the swordfish population.

## 6.2. INCREASE IN AVAILABILITY

The second hypothesis to explain the change in the indices of abundance is a change in availability. The availability of the fish may be understood as the density and distribution of the fish in relation to that of the distribution of the gear (Ward 2008). It is one of the key components of catchability, which can be defined as the proportion of animals in population caught by one unit effort. Other components of catchability are related to the fishing gear and the fishing operations. Because the increase was observed in all indices simultaneously, including indices external areas such as the index for the New Zealand longline fishery ([SAC-13-INF-M](#)), and in different gears, it is less likely that, if the increase is truly an increase catchability, it would be due to a technological change adopted in all those fleets at about the same time.

For longliners, several changes have been documented that may have increase the catchability for swordfish. The use of lightsticks may increase the catch rate 5-fold depending on the color of the light used (Hazin *et al.* 2005). There is no information of the use of lightstick for most fleets. The Japanese fleet may have started using lightsticks in the late 1990's (Ward and Hindmarsh, 2007). When available and included in the standardization of the CPUE data (*e.g.* for the New Zealand fleet), the index still showed an increase after the mid 2000's ([SAC-13-INF-M](#)). The ability to detect suitable habitats for swordfish may have contributed to the increase in catchability. The availability of satellite imagery increased in sophistication and decrease in price over time. Already in the mid 1970's, the Japanese fleet had access to sea surface temperature images. In the early 2000's ocean color images and sea surface height images were available for that fleet (Ward and Hindmarsh, 2007). Those data associated with the precise location of the vessel given by the global positioning system (available since the mid 1980's for the Japanese fleet), may help indicate the proximity to suitable swordfish habitat and assist in refining the fishing tactic. In addition, the use of Doppler profiler (available since the late 1980's for the Japanese fleet, Ward and Hindmarsh, 2007) may contribute to the decision making on gear deployment in relation to the currents.

The areas of high availability of swordfish seem to be frontal areas of high kinetic energy. In the HCS, mesoscale eddies and filaments advect cold nutrient-rich coastal water offshore, for hundreds of kilometers (Thiel *et al.* 2007). Eddy kinetic energy is stronger and more closely associated with the coast (~600 km) in the region between ~30°S and 38 °S, and away from the coast (>300 km) off Peru and ~30°S off Chile. Similar to other areas (*e.g.* the California Current System, Scales *et al.*, 2018), the highest CPUE for the Chilean longline fishery was associated with the highest frontal energy (measured by the encounter of the 17°C and 18°C) given by the intrusion of equatorial waters towards the southern area (south of 36°S) (Espíndola *et al.* 2009, Espíndola *et al.* 2011). However, swordfish seem to prefer the edges of the eddies (Espíndola *et al.* in published), where they fish as solitary predators. The eddies may accumulate nutrients or make them available in the photic zone increasing the primary and secondary productivity (Olson, 1991, Prants, 2022). The warm-core eddies seem particularly attractive for swordfish. In the Kuroshio current system, the swordfish CPUE in warm-core eddies is about 2-3 times higher than the cold-core eddies (Durán Gómez *et al.* 2020). The detection of those areas using technological tools may increase the catchability for swordfish, while changes in the environment that increase the amount of mesoscale eddies, may have the effect of increasing the availability of swordfish to both longline and gillnet simultaneously.

The availability of swordfish may have increased due to changes in the distribution and quantity of frontal structures such as eddies and especially warm-core eddies after the year 2000 as a result of oceanographic changes. Scales *et al.* (2018) proposed a method to quantify the strength and number of eddies and frontal areas, named collectively as attracting “Lagrangian coherent structures” (LCS). Using this method, the authors estimated catch rates and higher probability of capture in areas with higher number and stronger LCS. Future work should consider studying the dynamic of LCS and its relations to swordfish catch rates,

and the ENSO in the south EPO to understand weather there is support for the hypothesis of increase in availability.

### **6.3. INCREASE IN PRODUCTIVITY AND AVAILABILITY**

This hypothesis combines an increase in productivity, caused potentially by the increase in the preferred prey of swordfish, and an increase in availability due to changes in the environment.

### **6.4. INCREASE IN CONNECTIVITY**

The average density estimated by the spatiotemporal model of the longline catch and effort operational level data from Japan indicated that the spatial areas of high density (or availability) in the early period were disconnected ([SAC-13-INF-N](#)). This pattern supported Hinton and Deriso's hypothesis of at least three populations in the EPO, one in the north, one in the south and one in the equatorial area. From 1994 to 2009 there are areas of higher density (or availability) and a slight increase in connectivity among those areas. After 2010, the connectivity increases strikingly between the equatorial area and the south EPO. It is plausible that the connectivity with the WCPO might have increased as well. Preliminary analysis of that the density estimated from the catch and effort data from the Spanish longline fleet suggest a corridor of areas of high density and large average sizes in the southern oceans around 35°S. The S WCPO swordfish assessment ([SC17-SA-WP-04](#)) showed a marked increase in depletion from about 80% to about 40% of the dynamic B<sub>0</sub> from 2000 to 2010, which although coincident with increase in catches in the WCPO and EPO, also coincides with the increase in the EPO indices, which may suggest movement from the WCPO to the EPO. That assessment also considers catches in the EPO that take place in the overlapping management area between the IATTC and the WCPFC (south of 4°S and between 150°W and 130°W), which are part of the current stock assessment for the S EPO. The published genetic and genomic data is inconclusive about clear cut stock separation and even suggest similarities between swordfish collected in Australia and in Chile.

## **7. CONCLUSION**

The indices of abundance are generally treated as the main information that needs to be fitted well by an assessment model (Francis 2011), this is under the hypothesis that the population would decrease with fishing (and *vice versa*) and that the indices would detect the effect of fishing. The S EPO swordfish stock assessment departs considerably from this hypothesis, as the indices seem to indicate that the higher catches could be sustained due to increases in productivity or movement from the WCPO, or the indices are showing only changes in availability of swordfish, or a mix of these. The increase in productivity hypothesis is not supported by some of the composition data. This can be the result of model misspecification, which if addressed and once resolved may reconcile the data components. Alternative data sources may be needed to discriminate among those hypotheses. Regardless of the high uncertainty, all the models estimated that the stock did not breach the suggested biomass and fishing limit reference points, but may be approaching the target reference points. Thus, the stock should be closely monitored.

The review of external evidence suggests that the hypothesis of increase in productivity cannot be ruled out, as it seems that the extreme increase in jumbo squid may have favored the swordfish stock, perhaps even in detriment of other stocks (Alarcón-Muñoz et al 2008 suggest that decreases in the Chilean hake population, an important prey of jumbo squid in the region, may be due to the increase in jumbo squid). Here we modelled change in productivity as change in recruitment. The real process may be, however, connected to other parameters such as changes in adult natural mortality because the energy provided by the abundance of prey may translate in increase recruitment, survival, or changes in growth. If there is a real increase in abundance of swordfish in the south EPO and this increase is associated with the increase in jumbo squid, the management actions should consider the possibility of that source of energy decreasing in the future and the swordfish population returning to a lower productivity state.

The increases in the indices of abundance with the increase in catches was the feature that dominated the focus of this assessment. The models used to explore the hypothesis used to explain that pattern, as modelled here, however, were not as influential in the stock status as the sensitivity runs. If the natural mortality for the stock was lower in general, the stock would be experiencing higher fishing intensity and would be in a lower population size than the levels corresponding to the suggested LRPs. Natural mortality and potential changes in natural mortality due to increase in prey abundance should be explored in the future.

## **8. RESEARCH RECOMMENDATIONS**

The catch reporting needs to be improved for some CPCs such as central and south American nations. The catches need to be reported at minimum by gear, quarter, with indication of the area of origin and in the original unit they were recorded (by weight or by number), to avoid relying on arbitrary assumptions to partition it. Ideally, the catches should be reported on a 5 by 5 by month resolution, both in numbers and in weight, if those two units are recorded. The availability of both numbers and weight allows for the estimation of average weight in space and time, which is informative on both biological and fisheries processes.

Male and female swordfish differ not only in their life history parameters but also in their behavior and movement patterns (ref). The only sex-specific data available for this assessment were the data for the Chilean fleet. It is commendable that Chile has such a thorough sampling program. The other fleets should implement data collections by sex so aspects of the life history and specially of the movements and habitat utilization can be elucidated, to best model the growth, natural mortality and selectivity by sex. The Chilean conditional age-at-length data was not used in this assessment because the time-step chosen for the population dynamics was quarter while the data was available in an annual scale. In the future, the data could be desegregated into quarters and used to better estimate growth and natural mortality by sex and explore temporal changes in those parameters.

Other analyses should be conducted such as expanding the modeling of density into the WC Pacific Ocean, further studying changes in longline catch strategies and its influence in catchability and identifying favorable oceanographic conditions for high swordfish CPUE (specifically presence of warm-core eddies).

The indices of abundances were obtained from standardization of operational level or fine resolution catch an effort data. Some covariates that are known to affect the catch rates were not available, which may prevent the standardized CPUE to be a good representation of the population. The lack of effort in numbers of hooks for the Spanish fleet forced the use of number of sets as the effort measure. Other variables that may contribute to increase in catchability include the number and color of light sticks (refs), and the use of satellite services to find the ideal oceanographic conditions for high swordfish catch rates (ref).

Despite the lack of important fishing strategy catchability covariates, the increase shown in several types of indices of different fleets and gears raised the hypotheses of changes in availability. Conditions that maybe causing changes in availability need to be elucidated.

The composition data was influential in the results of some of the models. While length frequency data was available through the submission to the IATTC under the data provision resolution, there is no meta-data information associated with these data to understand the sampling, so the data could be better represented in the assessment model and in the standardization models. For example, the amount of length frequency data for the Spanish fleet equated to the catch in numbers, indicating that the values submitted had been raised to the catch total. However, the length frequency data showed different spatial distribution than the catches, with some high catch areas having no samples. It is necessary that the sampling

protocols and the raising procedure, as well as the sample sizes, be submitted to the IATTC. Some fleets have very limited samples that appear not to be representative of the catches, in those cases the sampling design should be revised, and the sample sizes increased.

This assessment showed that there are at least four hypotheses that can explain the paradoxical patterns of increasing indices of abundance with simultaneous increase in catches. The available data does not contain the information necessary to be able to indicate which hypothesis is more plausible. Other types of data may need to be collected with that aim. The connectivity between the WCPO stock and the EPO stock should be studied with a well-designed electronic tagging study, which should tag fish between longitudes 150°W to 130°W both in the equatorial areas and in the temperate areas around 35°S to 40°S. Long-term studies that should be considered for the stock are feasibility of a close-kin mark recapture to estimate abundance, movement, and stock structure.

Future work may consider the use of multispecies models, predator-prey models or models of Intermediate complexity for ecosystem assessments (*e.g.* Plaganyi et al 2022) to explore the hypotheses raised in this assessment. The influence of jumbo squid abundance on natural mortality and growth of swordfish, in addition to recruitment, should also be investigated to determine if it can reconcile the conflict between the composition data and the indices of abundance.

## 9. ACKNOWLEDGEMENTS

The staff is grateful to the national scientists and authorities of Chile, Spain, Japan, Korea, Ecuador, for sharing of confidential data and information, and collaborating in several studies supporting this assessment, and to the participants of the 1st Technical Workshop on Swordfish in the South EPO (SWO-01) for suggestions and recommendations.

## 10. REFERENCES

- Alarcón-Muñoz, R., Cubillos, L., Gatica, C. 2008. Jumbo squid (*Dosidicus gigas*) biomass off central Chile: effects on Chilean hake (*Merluccius gayi*). CalCOFI Rep., Vol. 49: 157-166/
- Arkhipkin, A., Argüelles, J., Shcherbich, Z., Yamashiro, C. Ambient temperature influence adult size and life span in jumbo squid *Dosidicus gigas*
- Barría Martínez, P., González Pizarro, A., Devia Cortés, Mora Opazo, S., Miranda Pérez, H., Barraza Sáez, A., Cerna Troncoso, F., Cid Mieres, L., Ortega Carrasco, J.C., 2019. Informe Final. Convenio de Desempeño 2018. Seguimiento Pesquerías Recursos Altamente Migratorios. Aspectos biológico pesqueros, año 2018. Instituto de Fomento Pesquero.
- Carvalho, F., Winker, H., Courtney, D., Kapur, M., Kell, L., Cardinale, M., Schirripa, M., Kitakado, T., Yemane, Y., Piner, K.R., Maunder, M.N., Taylor, I., Wetzel, C.R., Doering, K., Johnson, K.F., Methot, R.D. 2021. A cookbook for using model diagnostics in integrated stock assessments. Fisheries Research 240. doi.org/10.1016/j.fishres.2021.105959
- Cerna, J. F. 2009. Age and growth of the swordfish (*Xiphias gladius* Linnaeus, 1758) in the southeastern Pacific off Chile (2001). Latin American Journal of Aquatic Research 37(1): 59-69.
- Claramunt, G., G. Herrera, M. Donoso and E. Acuña. 2009. Spawning period and fecundity of swordfish (*Xiphias gladius*) caught in the southeastern Pacific. Latin American Journal of Aquatic Research 37(1): 29-41.
- Cope, J.M., Punt, A.E., 2011. Reconciling stock assessment and management scales under conditions of spatially varying catch histories. Fisheries Research 107: 22–38
- Csirke, J., Alegre, A., Argüelles, J., Guevara-Carrasco, R., Mariátegui, L., Segura, M., Tafúr, R. and Yamashiro, C. 2015 Main Biological and fishery aspects of the Jumbo squid in the Peruvian Humboldt Current



System. South Pacific Regional Fisheries Management Organisation. 3rd Meeting of the Scientific Committee SC-03-27

- DeMartini, E. E., J. H. Uchiyama, R. L. Humphreys Jr., J. D. Sampaga and H. A. Williams. 2007. Age and growth of swordfish (*Xiphias gladius*) caught by the Hawaii-based pelagic longline fishery. *Fishery Bulletin* 105: 356–367.
- Durán Gómez, G.S., Nagai, T., Yokawa, K. 2020. Mesoscale Warm-Core Eddies Drive Interannual Modulations of Swordfish Catch in the Kuroshio Extension System. *Front. Mar. Sci.* 7:680. doi: 10.3389/fmars.2020.00680
- Espíndola, F., Vega, R., Yáñez, E. 2009. Identification of the spatial-temporal distribution pattern of swordfish (*Xiphias gladius*) in the southeastern Pacific. *Latin American Journal of Aquatic Research*, 37(1): 43-57.
- Espíndola, F., Yáñez, E., Barbieri, M.A. 2011. El Niño Southern Oscillation and spatial-temporal variability of the nominal performances of swordfish (*Xiphias gladius*) in the southeastern Pacific. *Revista de Biología Marina y Oceanografía* 46(2): 231-242
- Evans, K., Abascal, F., Kolody, D., Sippel, T., Holdsworth, J., Maru, P. 2014. The horizontal and vertical dynamics of swordfish in the South Pacific Ocean. *Journal of Experimental Marine Biology and Ecology* 450: 55–67.
- Francis, R.I.C.C. 2011. Data weighting in statistical fisheries stock assessment models. *Canadian Journal of Fisheries and Aquatic Sciences* 68(6): 1124-1138. <https://doi.org/10.1139/f2011-025>.
- Goodyear, C. P. 1993. Spawning stock biomass per recruit in fisheries management: foundation and current use. In S. J. Smith, J. J. Hunt and D. Rivard [ed.] *Risk evaluation and biological reference points for fisheries management*. *Can. Spec. Publ. Fish. Aquat. Sci.* 120: 67-81.
- Guevara-Carrasco R., Bertrand A. (Eds.). 2017. *Atlas de la pesca artesanal del mar del Perú*. Edición IMARPE-IRD, Lima, Perú, 183 pp. Hinton and Deriso 1998
- Hazin, H.G., Hazin, F.H.V., Travassos, P., Erzini, K. 2005. Effect of light-sticks and electrolume attractors on surface-longline catches of swordfish (*Xiphias gladius*, Linnaeus, 1759) in the southwest equatorial Atlantic. *Fisheries Research* 72: 271–277.
- Hinton, M.G. and Maunder, M.N. 2012. Status of swordfish in the eastern Pacific Ocean in 2010 and outlook for the future. *IATTC Stock Assessment Report 12. Status of the tuna and billfish stocks in 2010*. Pag. 133 – 177
- Ibáñez, C.M., González, C., Cubillos, L. 2004. Dieta del pez espada *Xiphias gladius* Linnaeus, 1758, en aguas oceánicas de Chile central en invierno de 2003. *Invest. Mar., Valparaíso*, 32(2): 113-120.
- Lennert-Cody, C.E., Maunder, M.N., Aires-da-Silva, A., Minami, M. 2013. Defining population spatial units: Simultaneous analysis of frequency distributions and time series. *Fisheries Research* 139: 85– 92.
- Lin, Q., Zhu, J. 2020. Topology-based analysis of pelagic food web structure in the central and eastern tropical Pacific Ocean based on longline observer data. *Acta Oceanol. Sin.* 39 (6): 1–9.
- Lu, C. P., Chen, C. A., Hui, C. F., Tzeng, T. D., & Yeh, S. Y. 2006. Population genetic structure of the swordfish, *Xiphias gladius* (Linnaeus, 1758), in the Indian Ocean and west pacific inferred from the complete DNA sequence of the mitochondrial control region. *Zoological studies*, 45(2): 269-279.
- Martínez-Ortiz J, Aires-da-Silva AM, Lennert-Cody CE, Maunder MN (2015) The Ecuadorian Artisanal Fishery for Large Pelagics: Species Composition and Spatio-Temporal Dynamics. *PLoS ONE* 10(8): e0135136. doi:10.1371/journal.pone.0135136
- Maunder, M.N., Thorson, J.T., Xu, H., Oliveros-Ramos, R, Hoyle, S.D., Tremblay-Boyer, L. Lee, H.H., Kai, M., Chang, S.-K., Kitakado, T., Albertsen, C.M., Minte-Vera, C.V., Lennert-Cody, C.E., Aires-da-Silva, A.M.,

- Piner, K.R. 2020a. The need for spatio-temporal modeling to determine catch-per-unit effort based indices of abundance and associated composition data for inclusion in stock assessment models. *Fisheries Research* 229 <https://doi.org/10.1016/j.fishres.2020.105594>
- Mejuto, J., and B. García-Cortés. 2005. Update of scientific and technical information on the activity of the EU-Spanish surface longline fleet targeting the swordfish (*Xiphias gladius*) in the Pacific, with special reference to recent years: 2002 and 2003. Manuscript. Doc BSTC 2005, Lanzarote, Spain, June 26-27, 2005: 17 p.
- Methot, R.D., and Wetzel, C.R. 2013. Stock synthesis: a biological and statistical framework for fish stock assessment and fishery management. *Fisheries Research* 142: 86-99.
- Methot, R.D., and Wetzel, C.R., Taylor, I.G., and Doering, K. 2020. Stock Synthesis User Manual Version 3.30.15. NOAA Fisheries Seattle, WA. NOAA. Processed Report NMFS-NWFSC-PR-2020-05
- Methot, R.D., Taylor, I.G. 2011. Adjusting for bias due to variability of estimated recruitments in fishery assessment models. *Can. J. Fish. Aquat. Sci.* 68: 1744–1760
- Minte-Vera, C.V., Maunder, M.N., Xu, H., Valero, J.L. Lennert-Cody, C.E., Aires-da-Silva, A. 2020. Yellowfin tuna in the eastern Pacific Ocean, 2019: benchmark assessment. 11th meeting of the Scientific Advisory Committee. Document SAC-11-07. Available from: [https://www.iattc.org/Meetings/Meetings2020/SAC-11/Docs/\\_English/SAC-11-07-MTG\\_Yellowfin%20tuna%20benchmark%20assessment%202019.pdf](https://www.iattc.org/Meetings/Meetings2020/SAC-11/Docs/_English/SAC-11-07-MTG_Yellowfin%20tuna%20benchmark%20assessment%202019.pdf)
- Minte-Vera, C.V., Maunder, M.N., Aires-da-Silva, A. 2021. Auxiliary diagnostic analyses used to detect model misspecification and highlight potential solutions in stock assessments: application to yellowfin tuna in the eastern Pacific Ocean. *ICES Journal of Marine Science*. <https://doi.org/10.1093/icesjms/fsab213>
- Montecino, V., Lange, C.B. 2009. The Humboldt Current System: Ecosystem components and processes, fisheries, and sediment studies. *Progress in Oceanography* 83: 65–79
- Moore, B.R. 2020. Biology, stock structure, fisheries and status of swordfish, *Xiphias gladius*, in the Pacific Ocean – a review. NIWA Client Report 20200361WN. National Institute of Water and Atmospheric Research, Wellington, NZ. 46 p.
- Olson, D. B., Hitchcock, G.L., Mariano, A.J., Ashjian, C.J., Peng, G., Nero, R.W., Podestá, G. P. 1991. Life on the edge: marine life and fronts. *Oceanography* 7(2): 52-60.
- Patterson, T., Evans, K., Hillary, R. 2021. Broadbill swordfish movements and transition rates across stock assessment spatial regions in the western and central Pacific. Western and Central Pacific Fisheries Commission. Scientific Committee Seventeenth Regular Session. WCPFC-SC17-2021/SA-IP-17
- Plaganyi, E., Blamey, L.K., Rogers, J.G.D., Tulloch, V.J.D. 2022. Playing the detective: Using multispecies approaches to estimate natural mortality rates. *Fisheries Research* 249: 106229. <https://doi.org/10.1016/j.fishres.2022.106229>
- Prants, S.V. 2022. Marine life at Lagrangian fronts. *Progress in Oceanography*. 204: 102790. <https://doi.org/10.1016/j.pocean.2022.102790>
- Ramos-Cartelle, A., Fernández-Costa, J., García-Cortés, B., Mejuto, J. 2021. Updated standardized catch rates for the north Atlantic stock of swordfish (*Xiphias gladius*) from the Spanish surface longline fleet for the period 1986-2019. SCRS/2021/087 Collect. Vol. Sci. Pap. ICCAT, 78(7): 94-108
- Reeb, C.A, Arcangeli, L., Block, B.A. 2000. Structure and migration corridors in Pacific populations of the swordfish *Xiphias gladius*, as inferred through analyses of mitochondrial DNA. *Marine Biology* 136: 1123-1131.

- Scales, K.L., Hazen, E.L., Jacox, M.G., Castruccio, F., Maxwelle, S.M., Lewison, R.L., Bograd, S.J. 2018. Fisheries bycatch risk to marine megafauna is intensified in Lagrangian coherent structures PNAS 7362–7367.
- Sepulveda, C.A., Wang, M., Aalbers, S.A., Alvarado-Bremer, J.R. 2020. Insights into the horizontal movements, migration patterns, and stock affiliation of California swordfish. *Fisheries Oceanography* 29:152–168.
- Thiel, M., Macaya, E.C., Acuña, E., Arntz, W.E. et al. 2007. The Humboldt current system of northern and central Chile: Oceanographic processes, ecological interactions and socioeconomic feedback. *Oceanography and Marine Biology: An Annual Review*, 45: 195-344
- Uchiyama, J.H., E.E. DeMartini and H.A. Williams. 1999. Length-weight interrelationships for swordfish, *Xiphias gladius* L., caught in the central north Pacific. NOAA-TM-NMFS-SWFSC-284, 82 p.
- Ward, P., Hindmarsh, S. 2007. An overview of historical changes in the fishing gear and practices of pelagic longliners, with particular reference to Japan's Pacific fleet. *Review Fish Biology and Fisheries* 17:501–516. doi 10.1007/s11160-007-9051-0
- Waterhouse, L., Sampson, D.B., Maunder, M., Semmens, B.X. 2014. Using areas-as-fleets selectivity to model spatial fishing: asymptotic curves are unlikely under equilibrium conditions. *Fisheries Research* 158:15-25. <https://doi.org/10.1016/j.fishres.2014.01.009>
- Xu, H., Maunder, M.N., Minte-Vera, C., Valero, J.L., Lennert-Cody, C., Aires-da-Silva, A. 2020. Bigeye tuna in the eastern Pacific Ocean, 2019: benchmark assessment. Inter-American Tropical Tuna Commission. 11th meeting of the Scientific Advisory Committee. Document SAC-11-06. Available from: [https://www.iattc.org/Meetings/Meetings2020/SAC-11/Docs/\\_English/SAC-11-06-MTG\\_Bigeye%20tuna%20benchmark%20assessment%202019.pdf](https://www.iattc.org/Meetings/Meetings2020/SAC-11/Docs/_English/SAC-11-06-MTG_Bigeye%20tuna%20benchmark%20assessment%202019.pdf)
- Zambrano-Zambrano, R.W., Mendoza-Moreira, P.E., Gómez-Zamora, W., Varela, J.L, 2019. Feeding ecology and consumption rate of broadbill swordfish (*Xiphias gladius*) in Ecuadorian waters. *Marine Biodiversity*. 49:373–380
- Zeidberg, L.D., Robison, B.H. 2007. Invasive range expansion by the Humboldt squid, *Dosidicus gigas*, in the eastern North Pacific. 104 (31) 12948-12950. <https://doi.org/10.1073/pnas.0702043104>

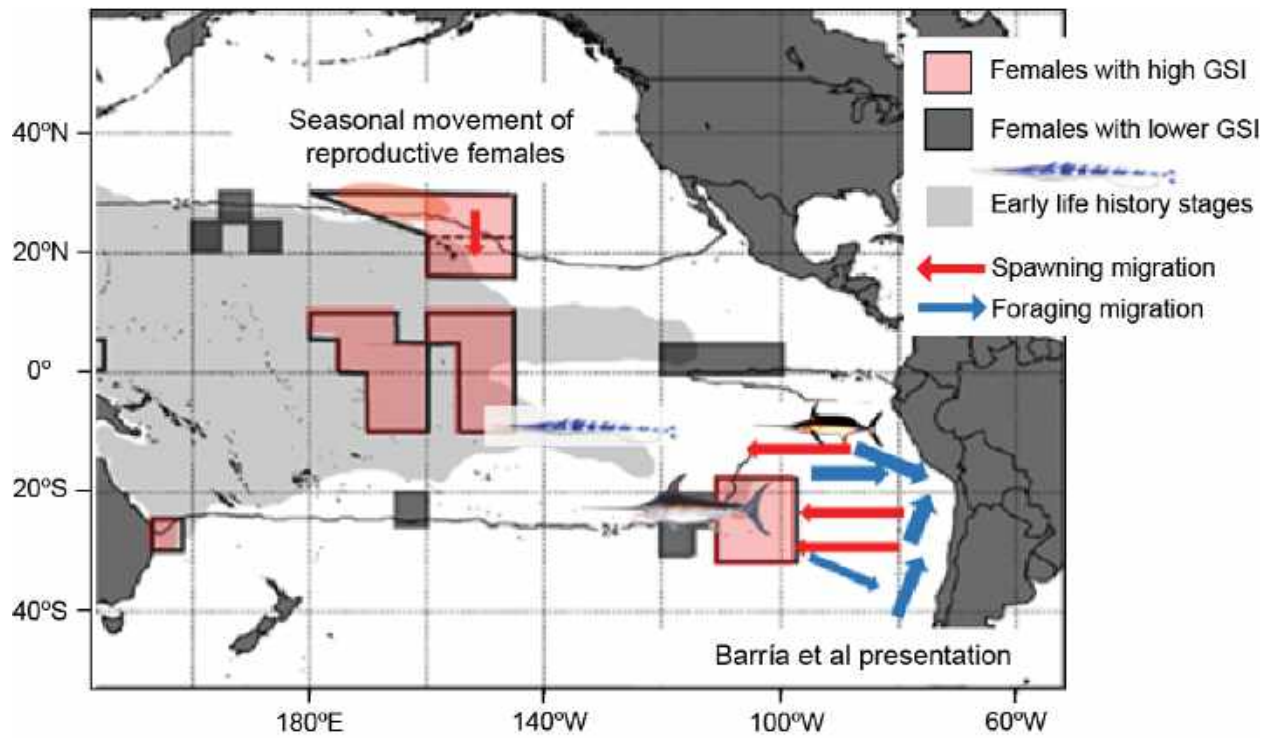


**FIGURE 1.** Conceptual model for the S EPO swordfish (Barría Martínez *et al.* 2020) overlaid on a map of known spawning and early life history areas (compiled by Lu *et al.* 2016).

DRAFT

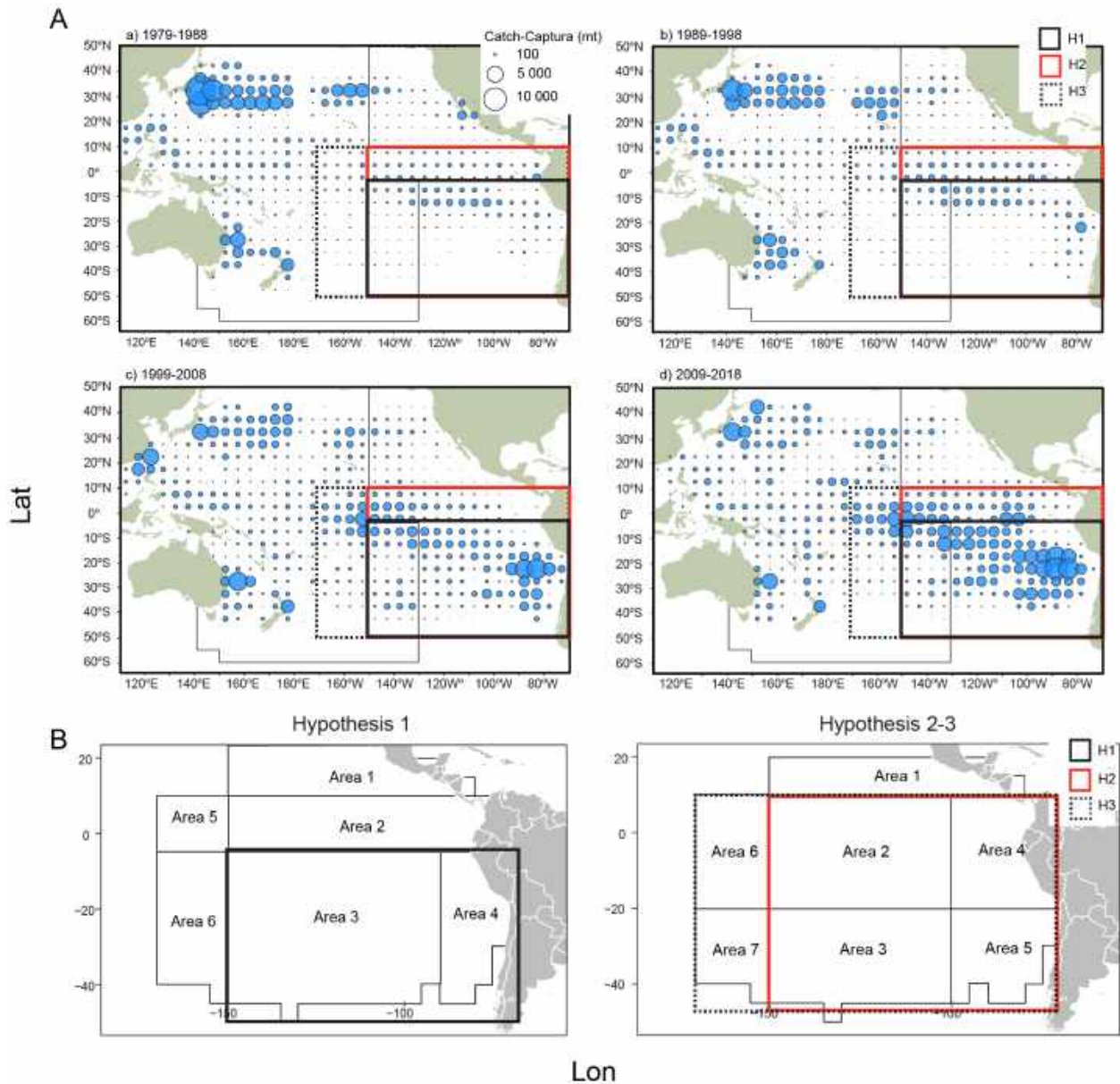


**FIGURE 2. A:** Map of distant water longline catches (mt) of swordfish, *Xiphias gladius*, by decade and 5° square from the Pacific Ocean, a) 1979–1988, b) 1989–1998, c) 1999–2008, d) 2009–2018 compiled by Moore (2021) overlaid with the regions corresponding to the three stock structure assumptions. **B:** Areas used for fishery definitions (Table 2) for each stock structure hypothesis. The areas for H1 are the same as in the 2011 assessment. The areas for H2 are based on tree analyses of the length frequencies, which are extended into the WCPO for H3.

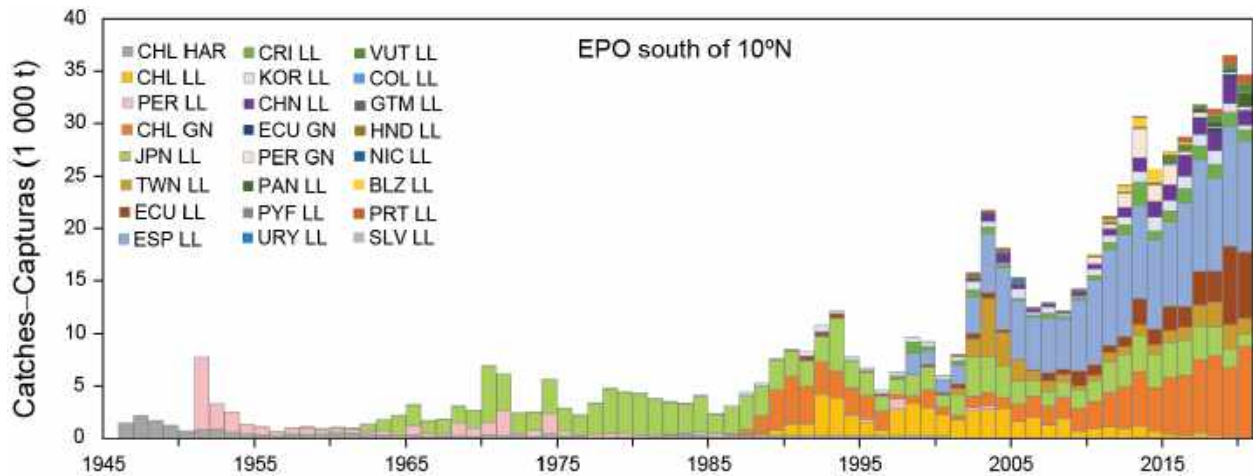


**FIGURE 3.** Annual catches of swordfish in the EPO south of 10°N in weight by fishing gear and CPC corresponding included in the stock assessment of swordfish for the south EPO in 2022. The CPC abbreviations are: BLZ – Belize, CHL – Chile, CHN – China, COL - Colombia, CRI – Costa Rica, ECU – Ecuador, ESP – Spain, GTM – Guatemala, HND – Honduras, JPN – Japan, KOR – Korea, NIC – Nicaragua, PAN – Panamá, PER – Perú, PRT – Portugal, PYF – French Polynesia, SLV – El Salvador, TWN – Chinese Taipei, URY – Uruguay, VUT – Vanuatu. The gear abbreviations are HAR – Harpoon, LL – Longline, GN – Gillnet.



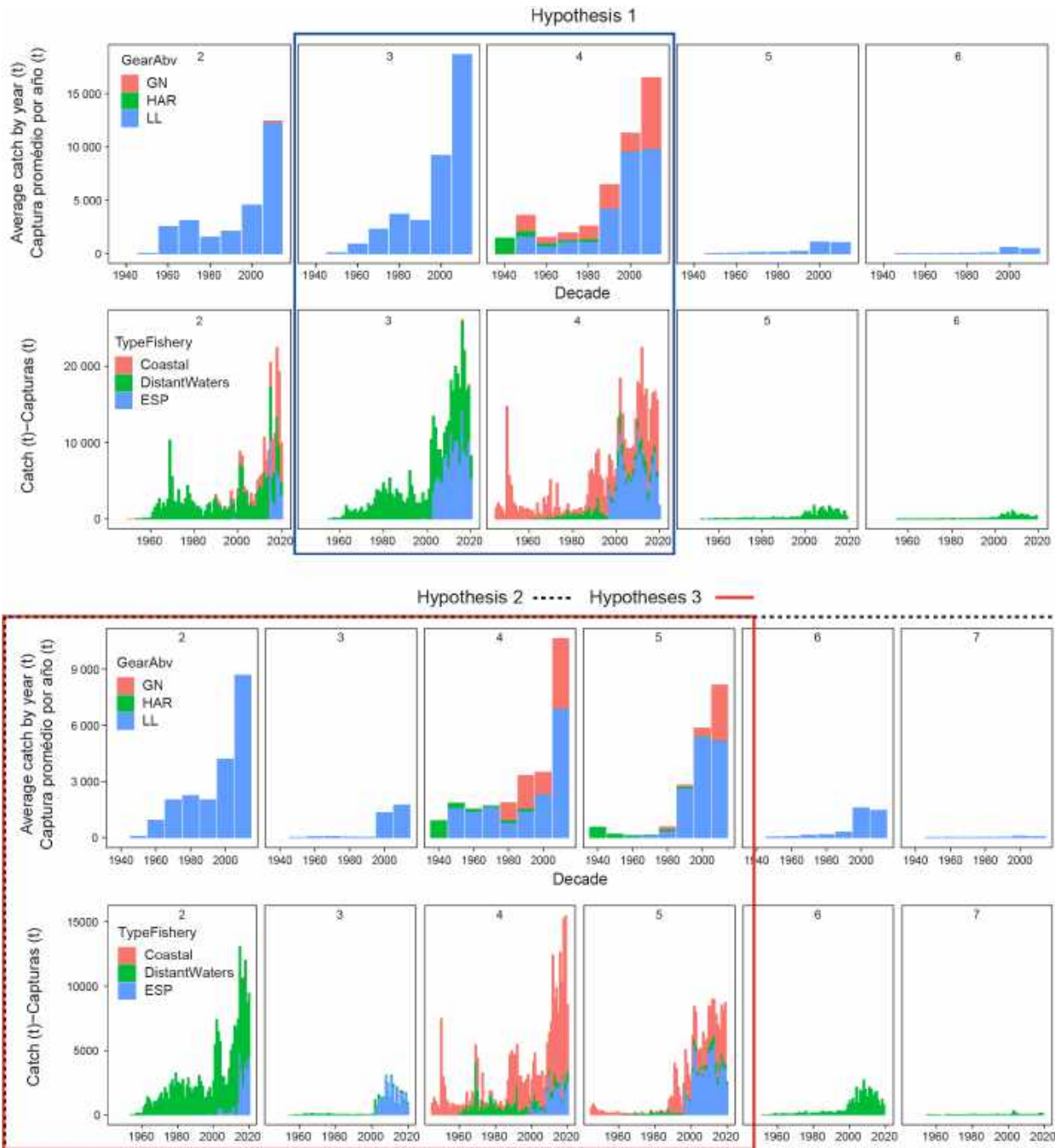


**FIGURE 4.** Catches in weight by fishing gear and type of fishery corresponding to the three stock-structure hypotheses, areas for fishery definitions (Table 2) and neighbor areas for the stock assessment of swordfish for the south EPO in 2022. The rectangles indicate the catches included in each stock structure hypothesis.

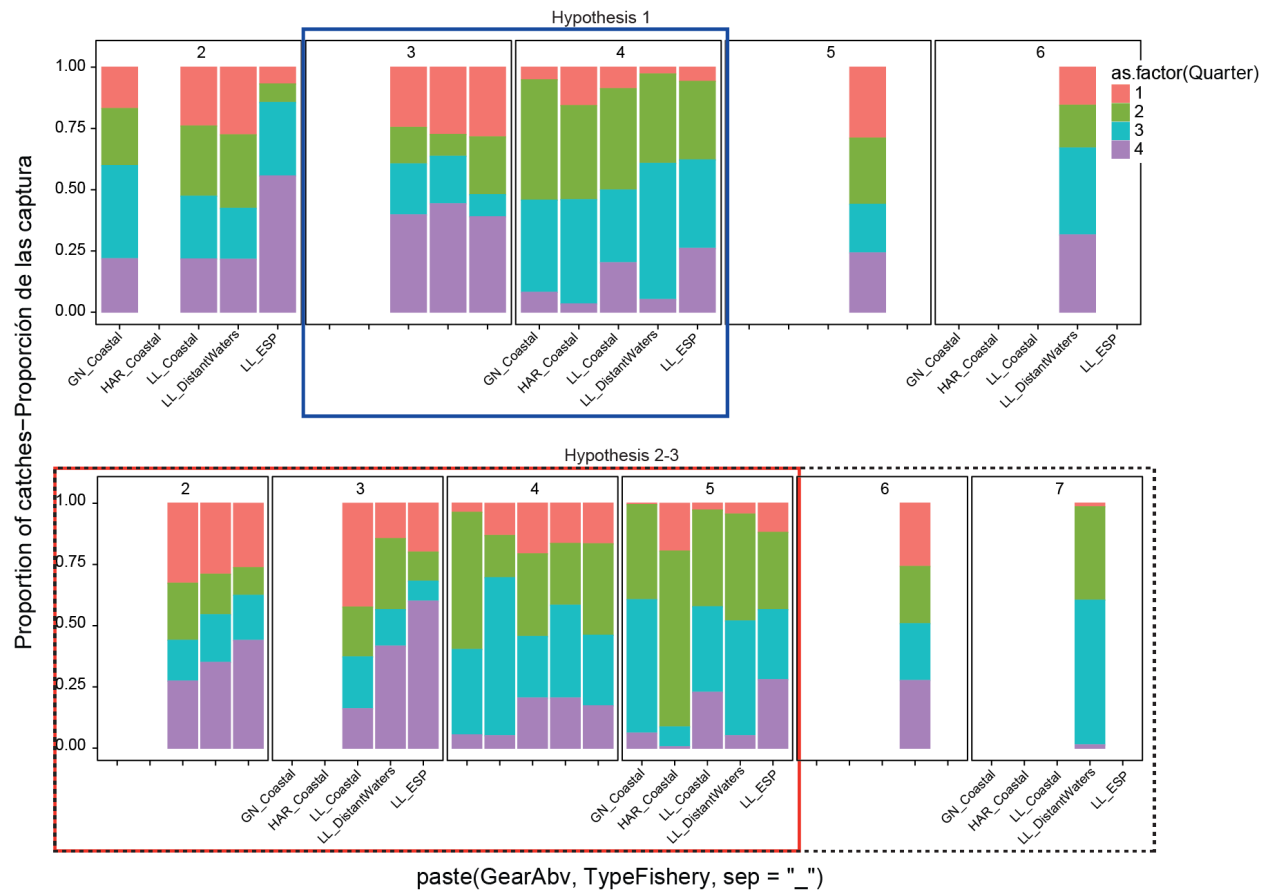


**FIGURE 5.** Seasonality of the catches in weight by fishing gear and type of fishery corresponding to the stock structure hypotheses, areas for fishery definitions (Table 2) and neighboring areas for the stock assessment of swordfish for the south EPO in 2022.

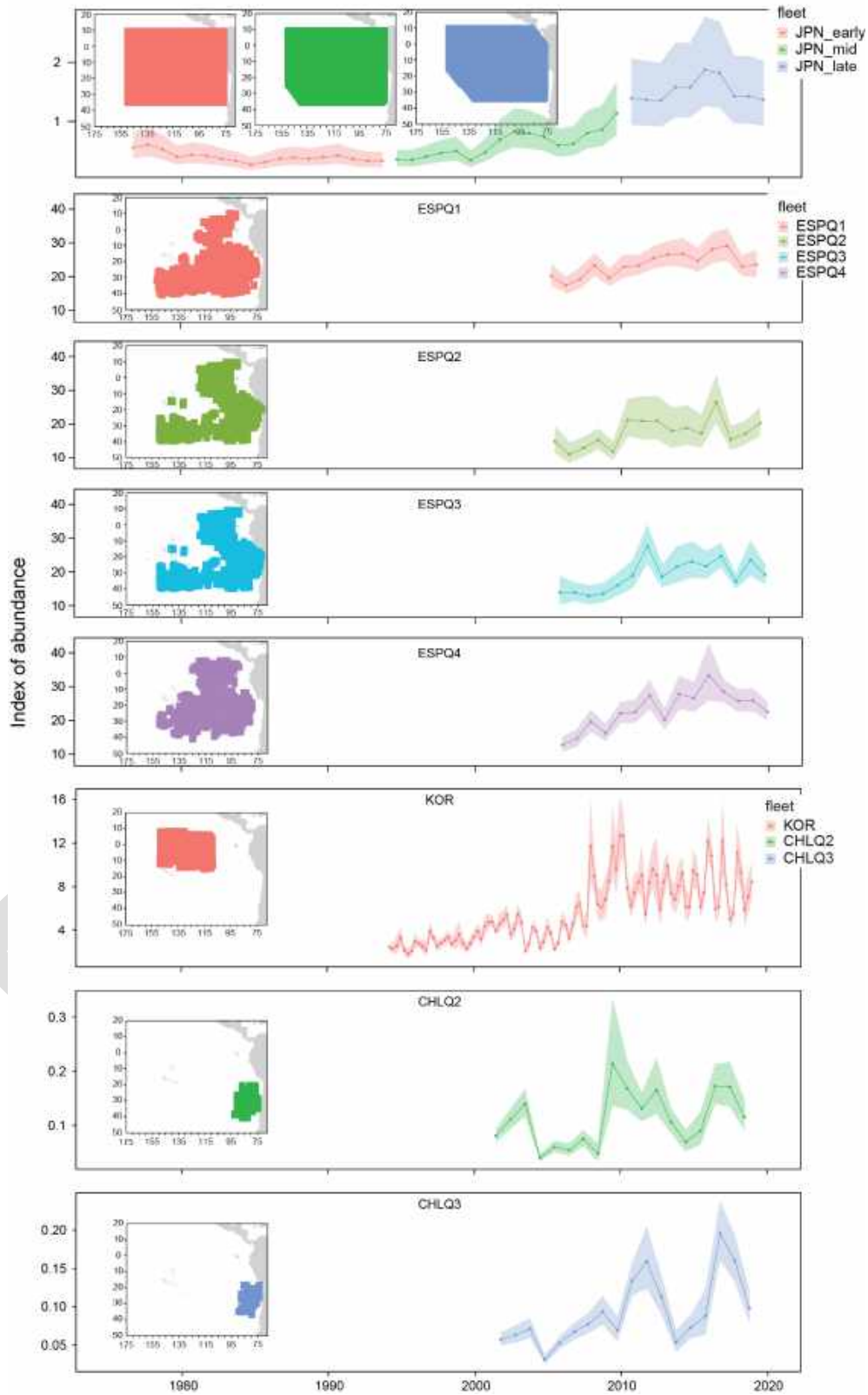
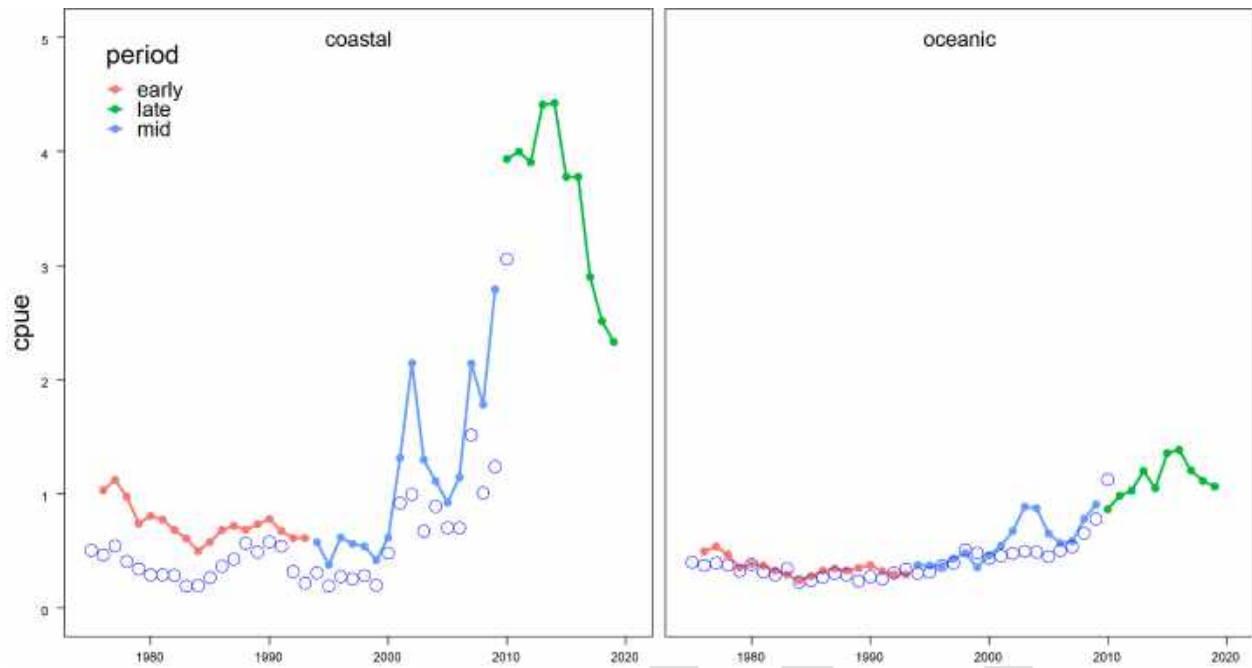
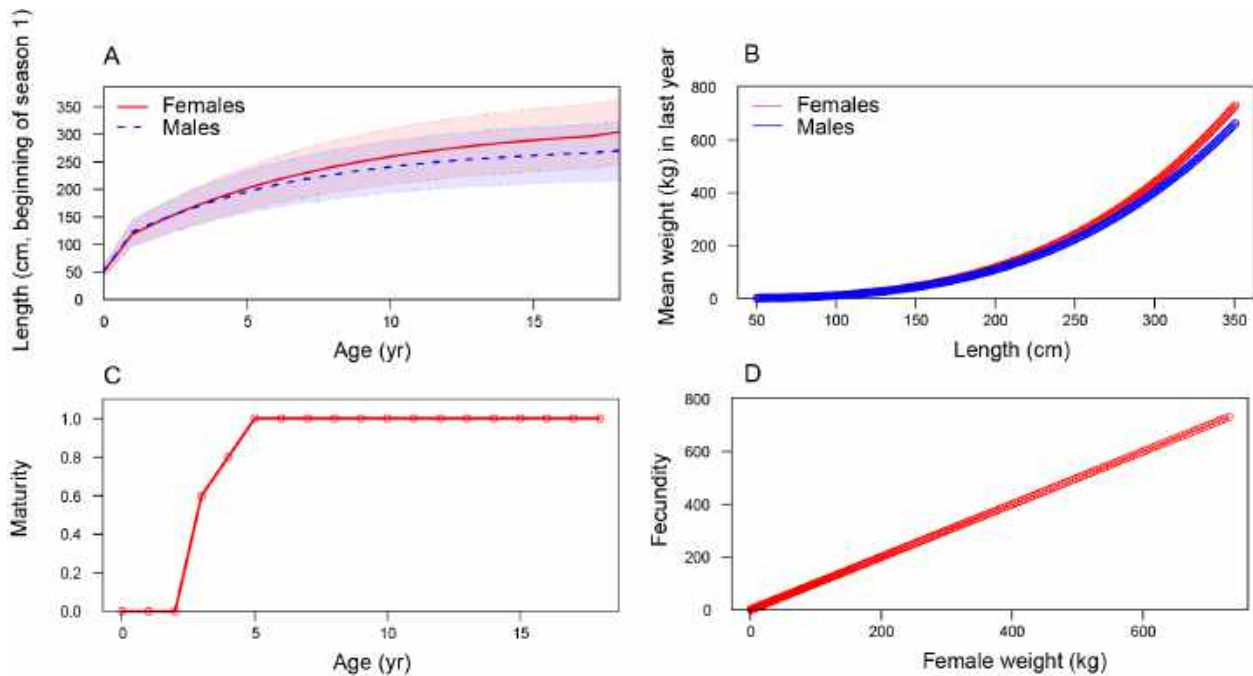


FIGURE 6. Extrapolation maps and time-series for each index.



**FIGURE 7.** Comparison of the Japanese indices from the 2011 assessment and from SAC-13-INF-M, aggregated into the coastal and offshore area.

DRAFT



**FIGURE 8.** Biological assumptions for the swordfish assessment in the south EPO. **A:** Assumed mean length at age for males and females, the shaded region represents variation in length-at-age, assuming a CV = 10% (mean  $\pm$  1.96 standard deviations). **B:** Length-weight relationship for males and females. **C:** Maturity at age for females. **D:** Fecundity at age for females

DRAFT

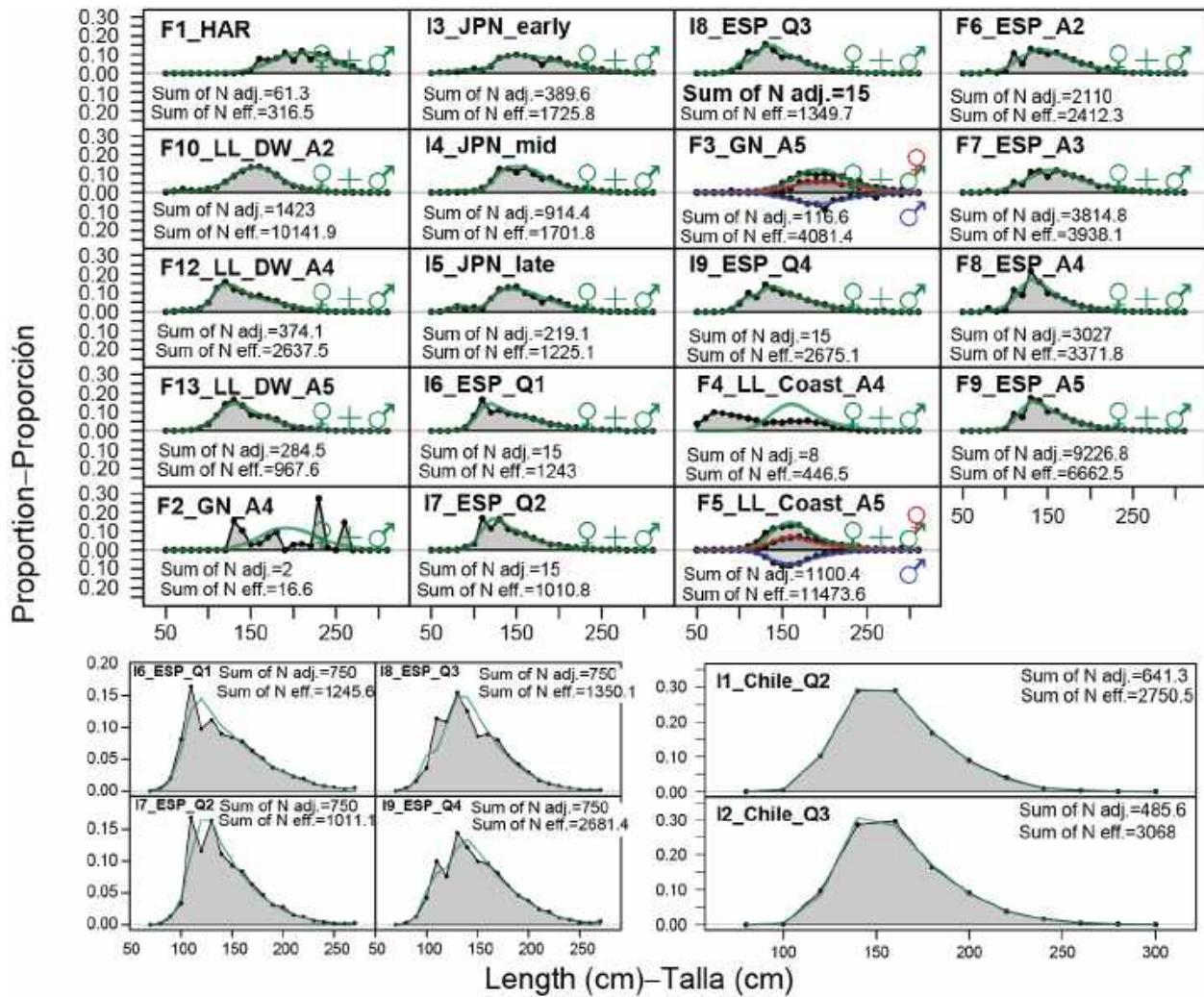


**FIGURE 9a.** Average length compositions weighted by the sample sizes associated with fisheries and indices. The observed values are shown as shaded area and the values predicted by the M0 model are shown as lines.



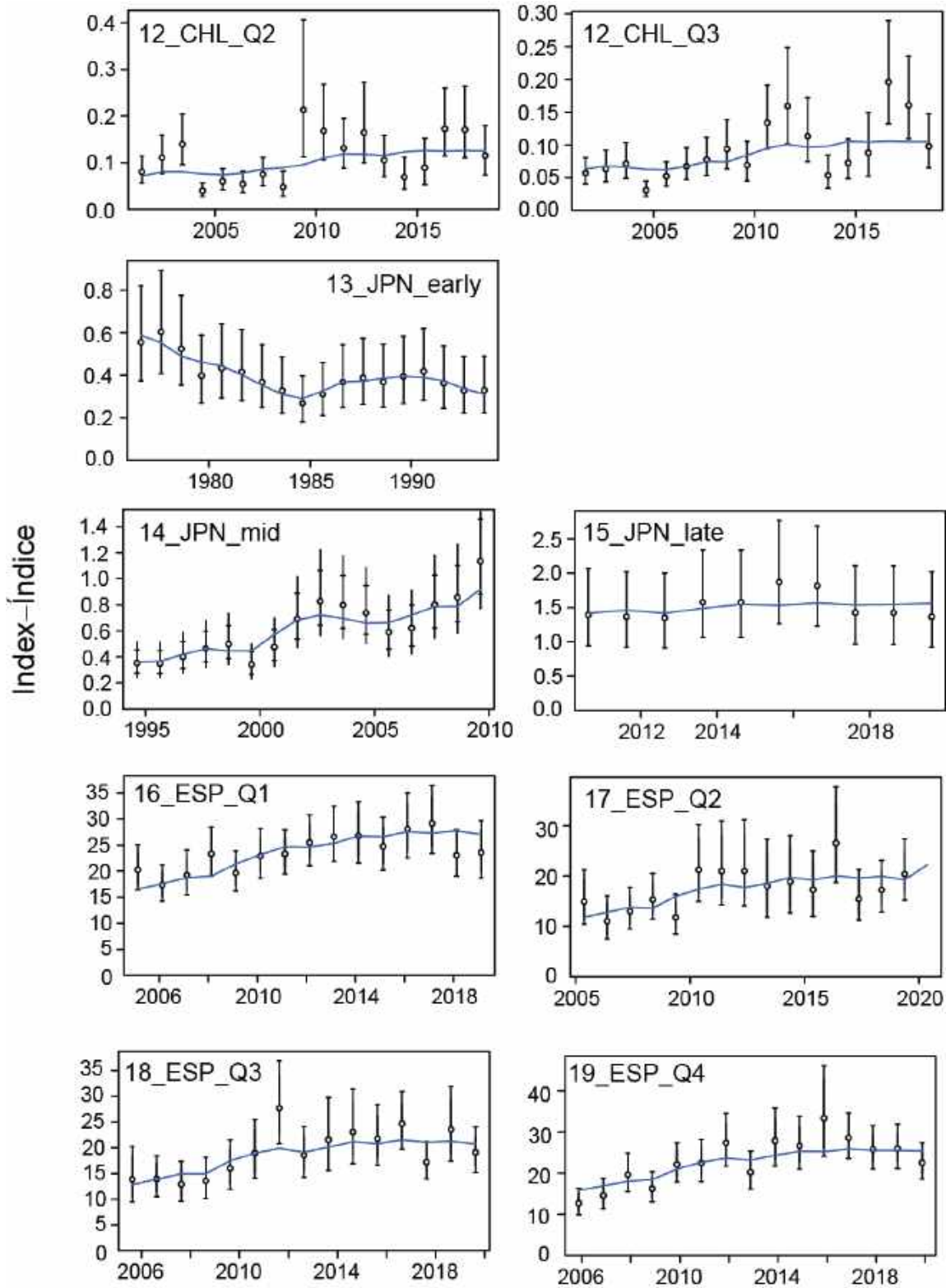


**FIGURE 9b.** Model fits to the CPUE-based indices of abundance by the reference model. The blue line represent the estimated indices, the circles are the observed CPUE values, and the vertical lines represent the uncertainty in the observations.

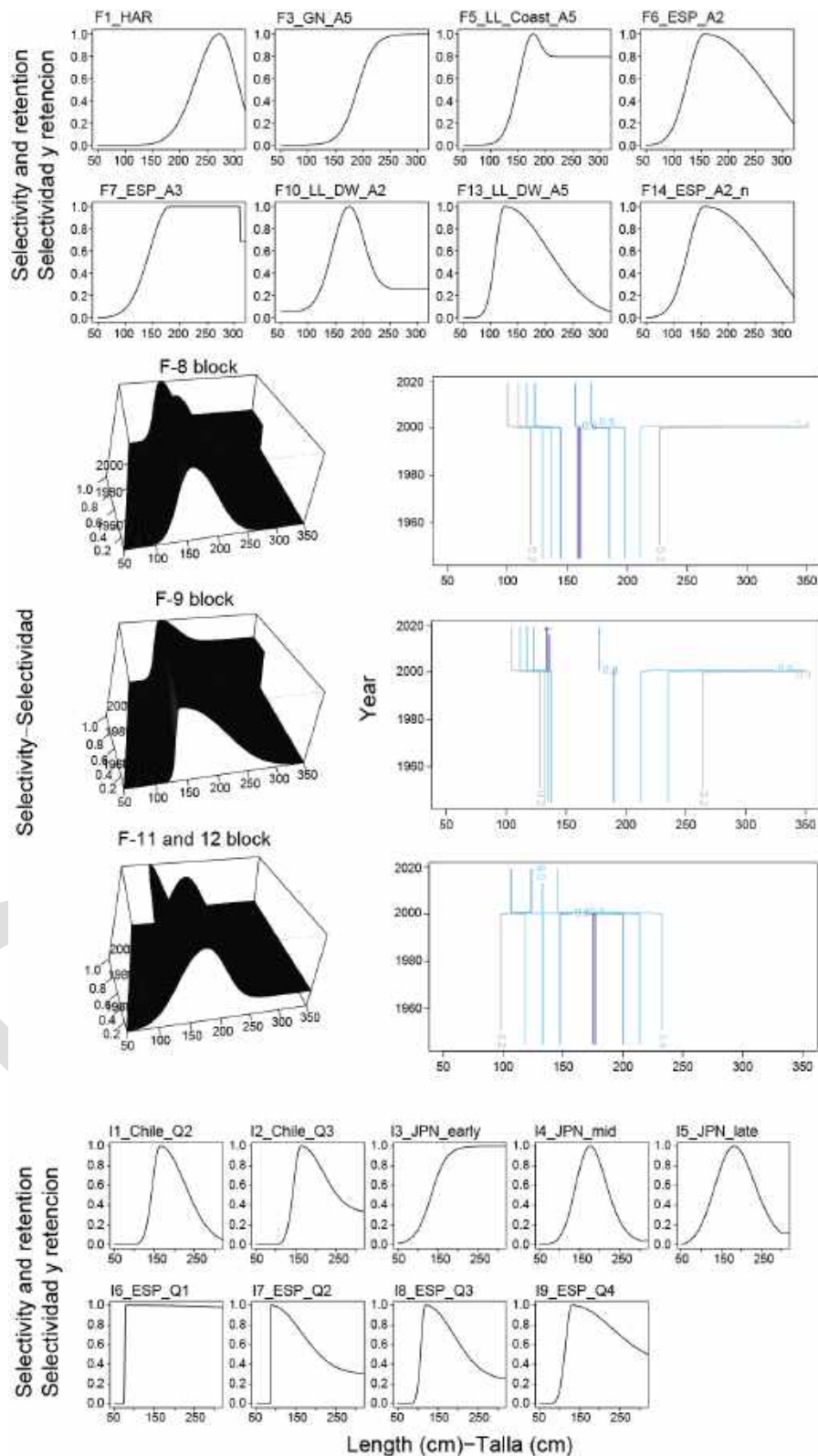
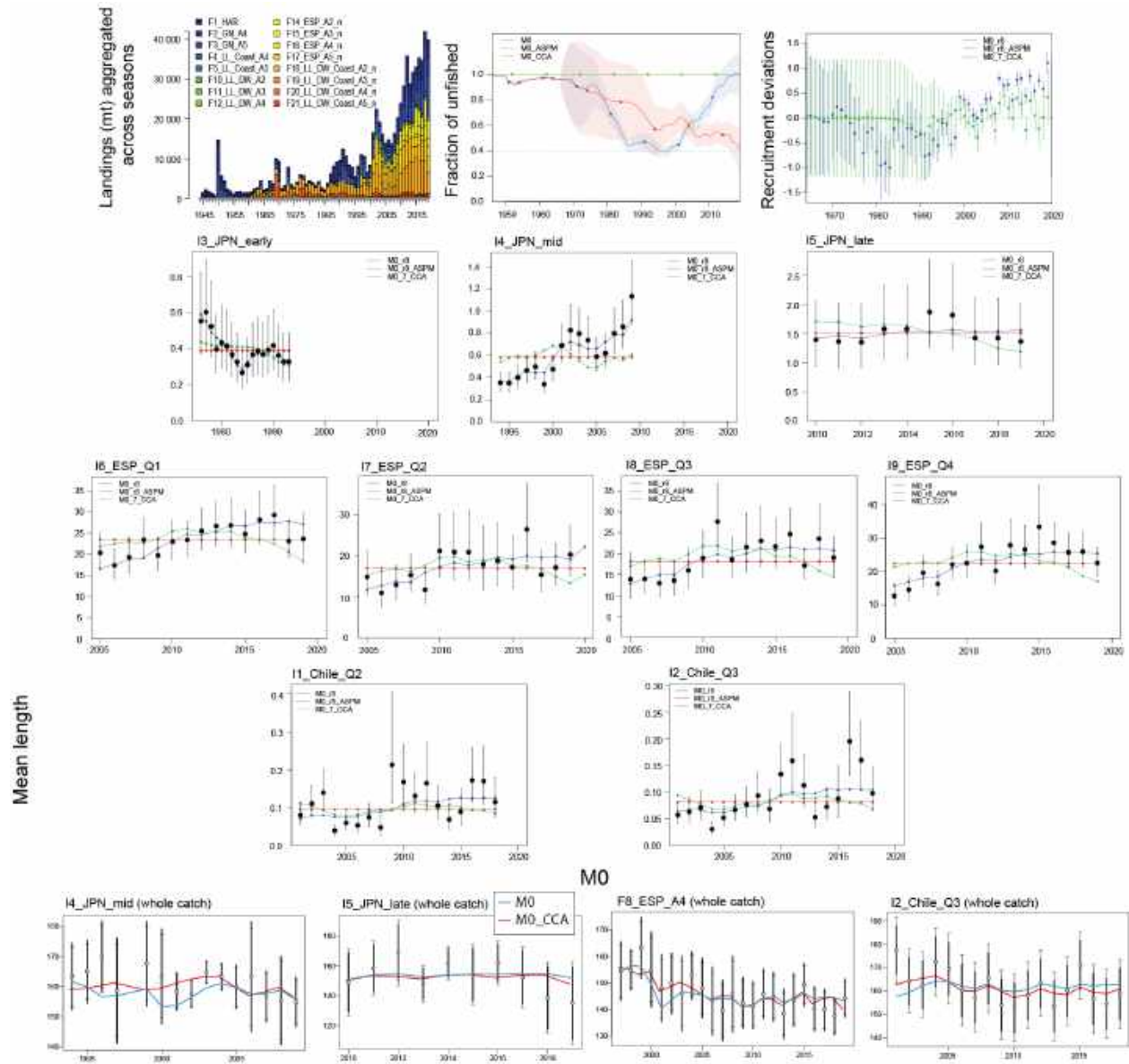
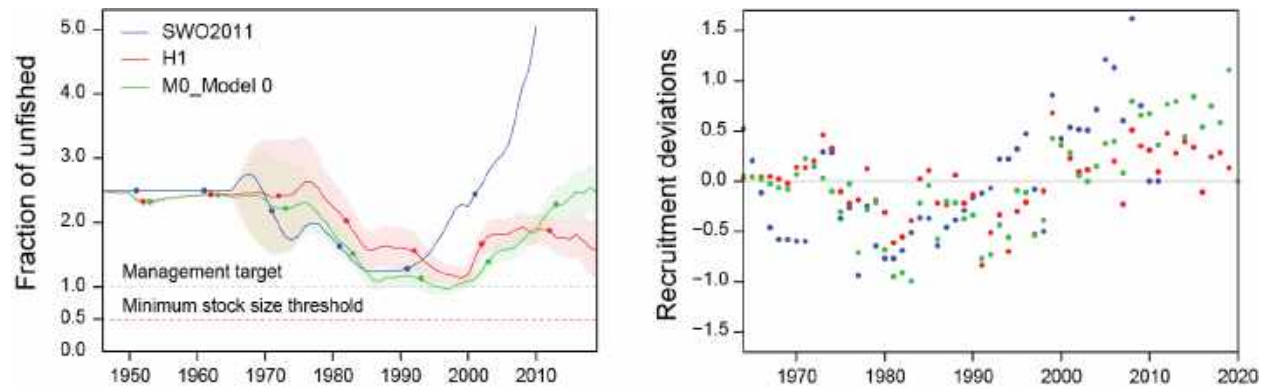


FIGURE 10. Selectivity functions estimated from the reference model M0, for fisheries and for indices.



**FIGURE 11.** Spawning biomass, recruitment deviations, fits to the indices for abundance for the reference model, and age-structured production and catch-curve diagnostics.



**FIGURE 12.** Estimated spawning biomass, recruitment deviations, for the 2011 assessment, update model and M0 model.

DRAFT

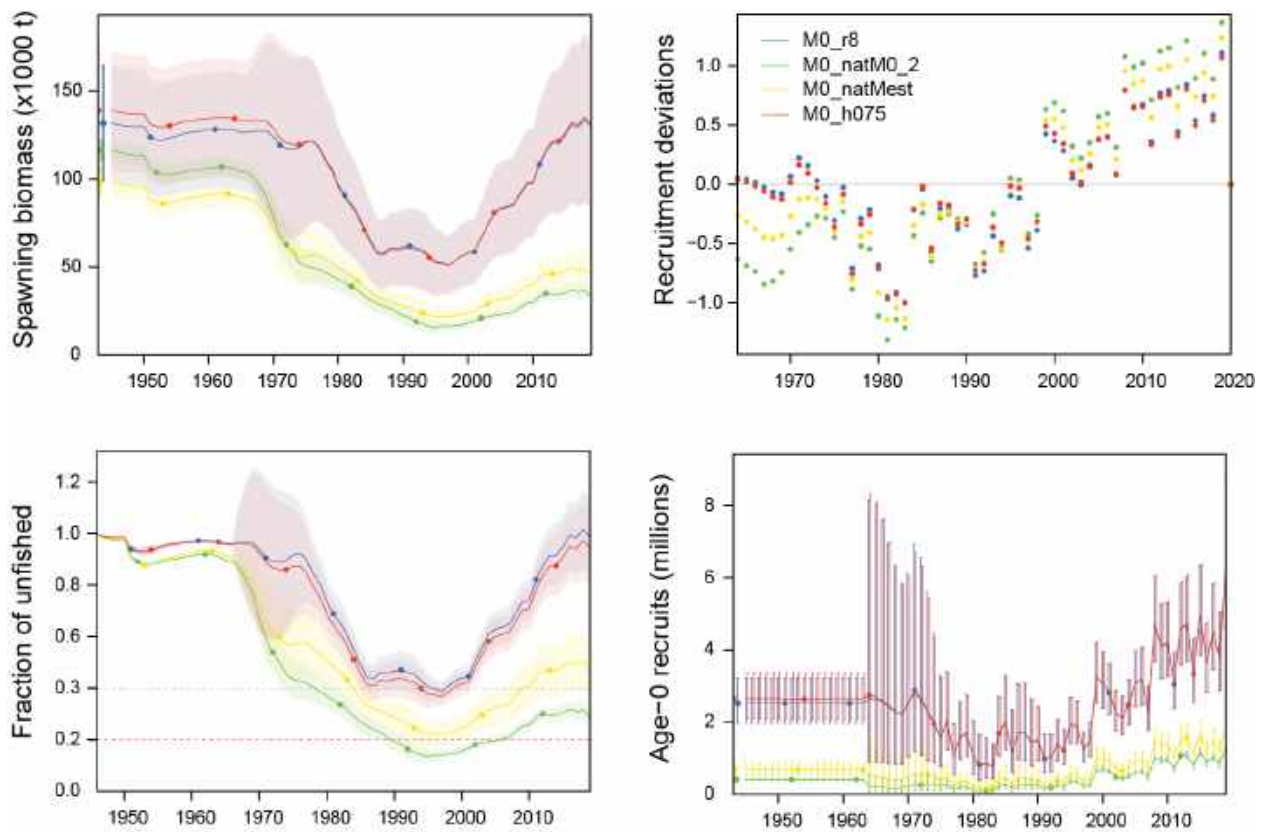


**FIGURE 13.** Estimated spawning biomass, recruitment deviations, depletion and recruitment estimate for the M0 reference model, estimate natural mortality model, M=0.2 and h=0.75 sensitivity models.



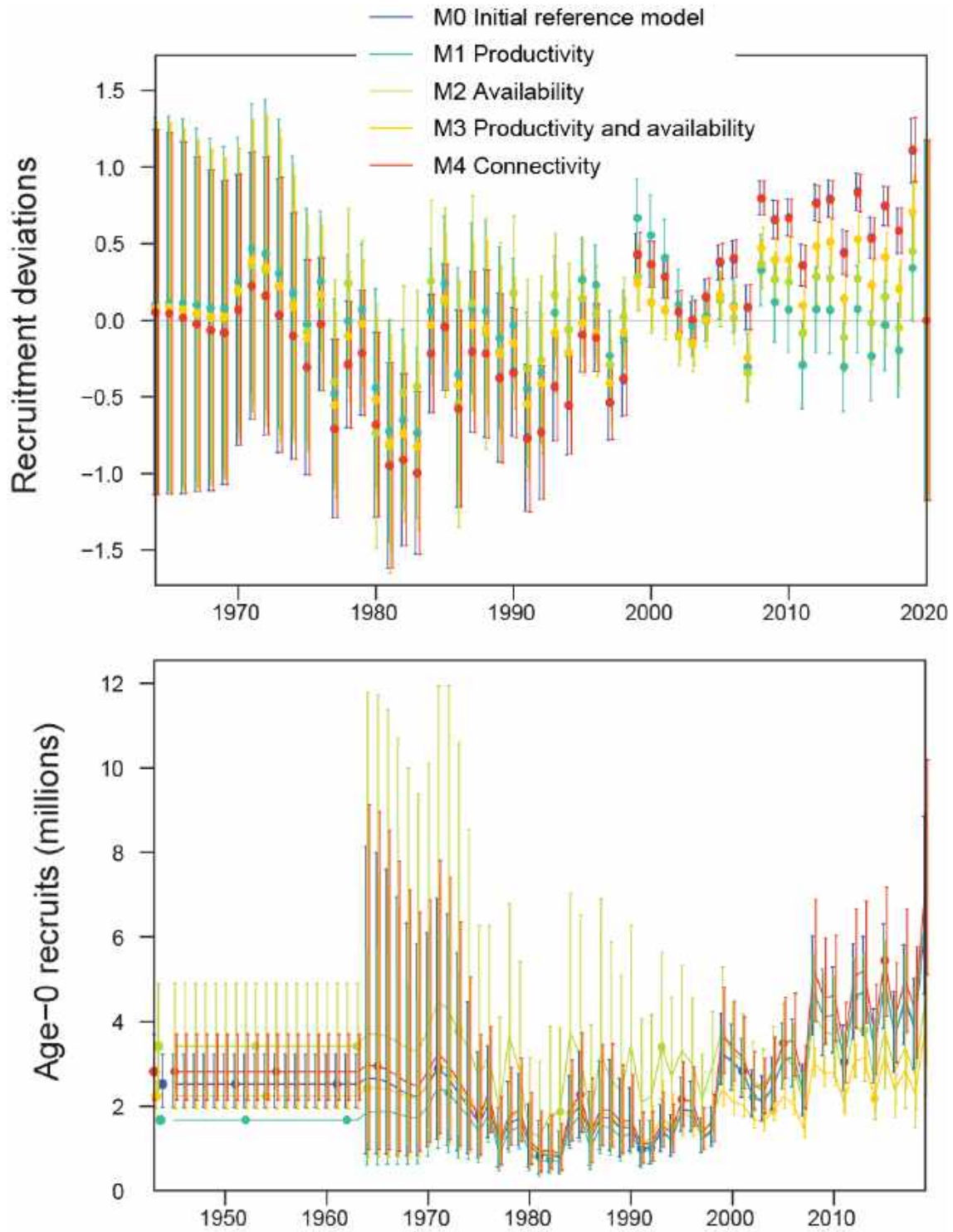


**FIGURE 14.** Top: recruitment deviations, Bottom: absolute recruitment estimates for the M0 initial reference model, and the models corresponding to the four hypotheses that explain the simultaneous increase in indices of abundance and catches.

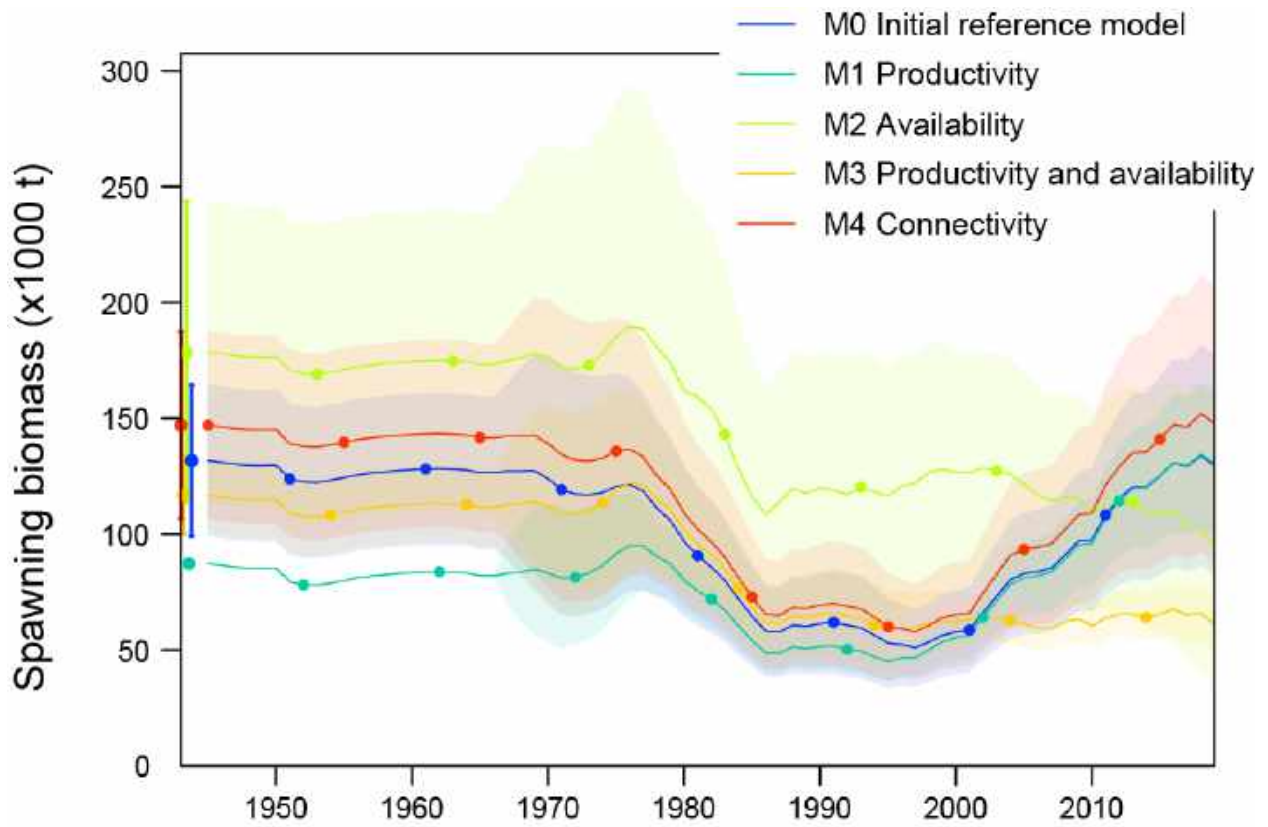


**FIGURE 15.** Spawning biomass for the M0 initial reference model, and the models corresponding to the four hypotheses that explain the simultaneous increase in indices of abundance and catches.



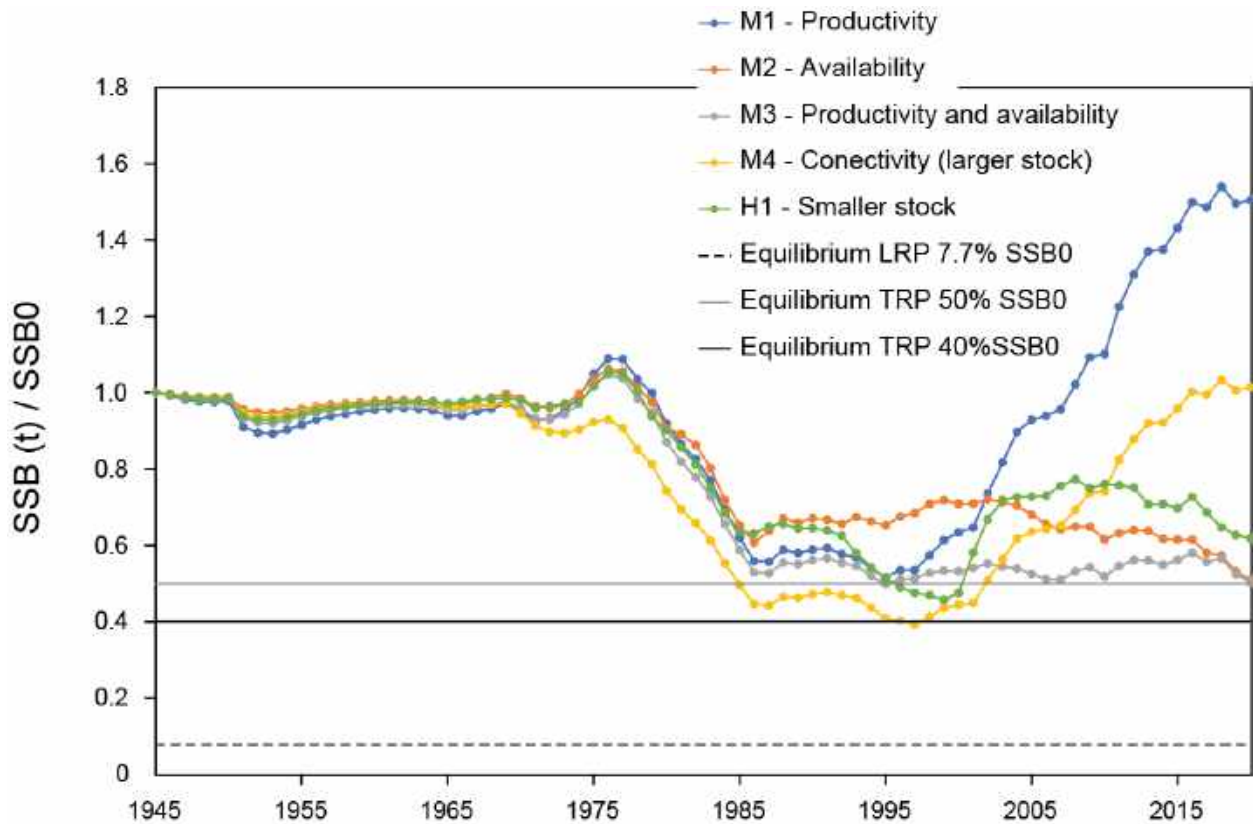


**FIGURE 16.** Ratio of the estimated spawning stock biomass and the virgin spawning stock biomass (equilibrium) for the models corresponding to the four hypotheses that explain the simultaneous increase in indices of abundance and catches and the model corresponding to the stock structure hypothesis H1 (north boundary at 5°S). Note that M4 corresponds to the stock structure hypothesis H3 (western boundary at 170°W).

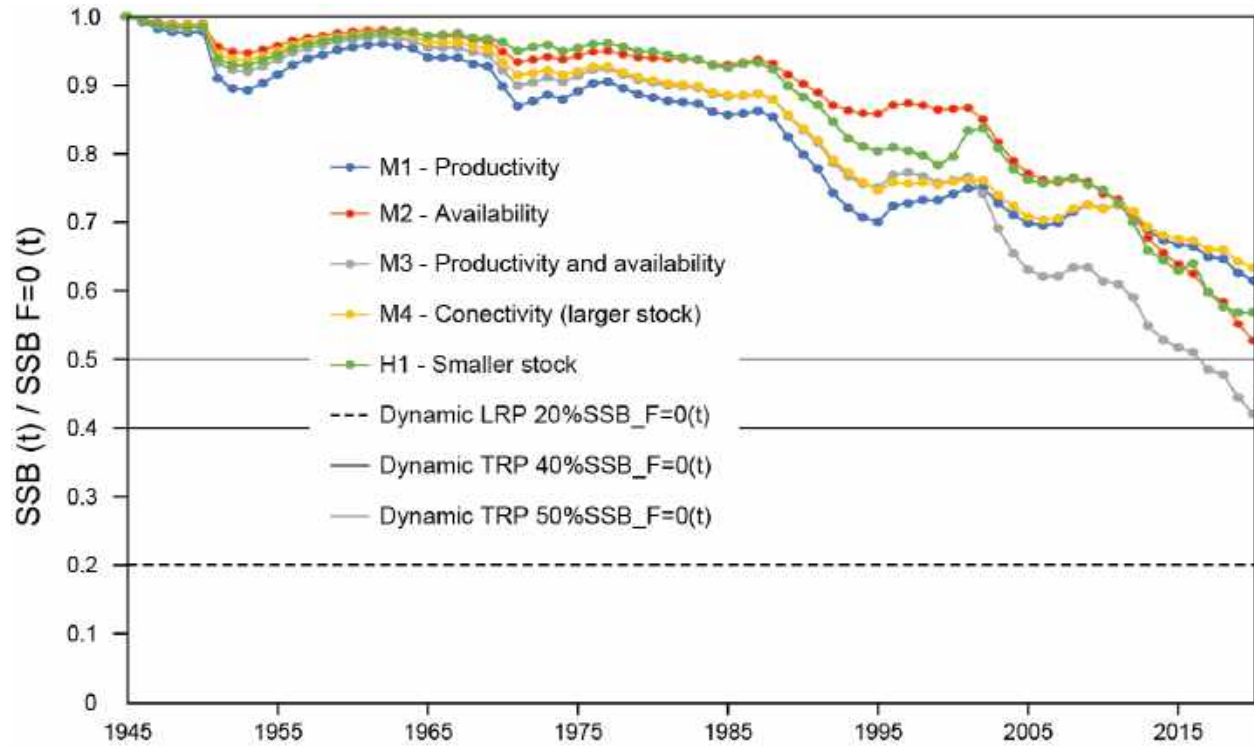


**FIGURE 17.** Ratio of the estimated spawning stock biomass and spawning stock biomass with no fishing (dynamic) for the models corresponding to the four hypotheses that explain the simultaneous increase in indices of abundance and catches and the model corresponding to the stock structure hypothesis H1 (north boundary at 5°S). Note that M4 corresponds to the stock structure hypothesis H3 (western boundary at 170°W).

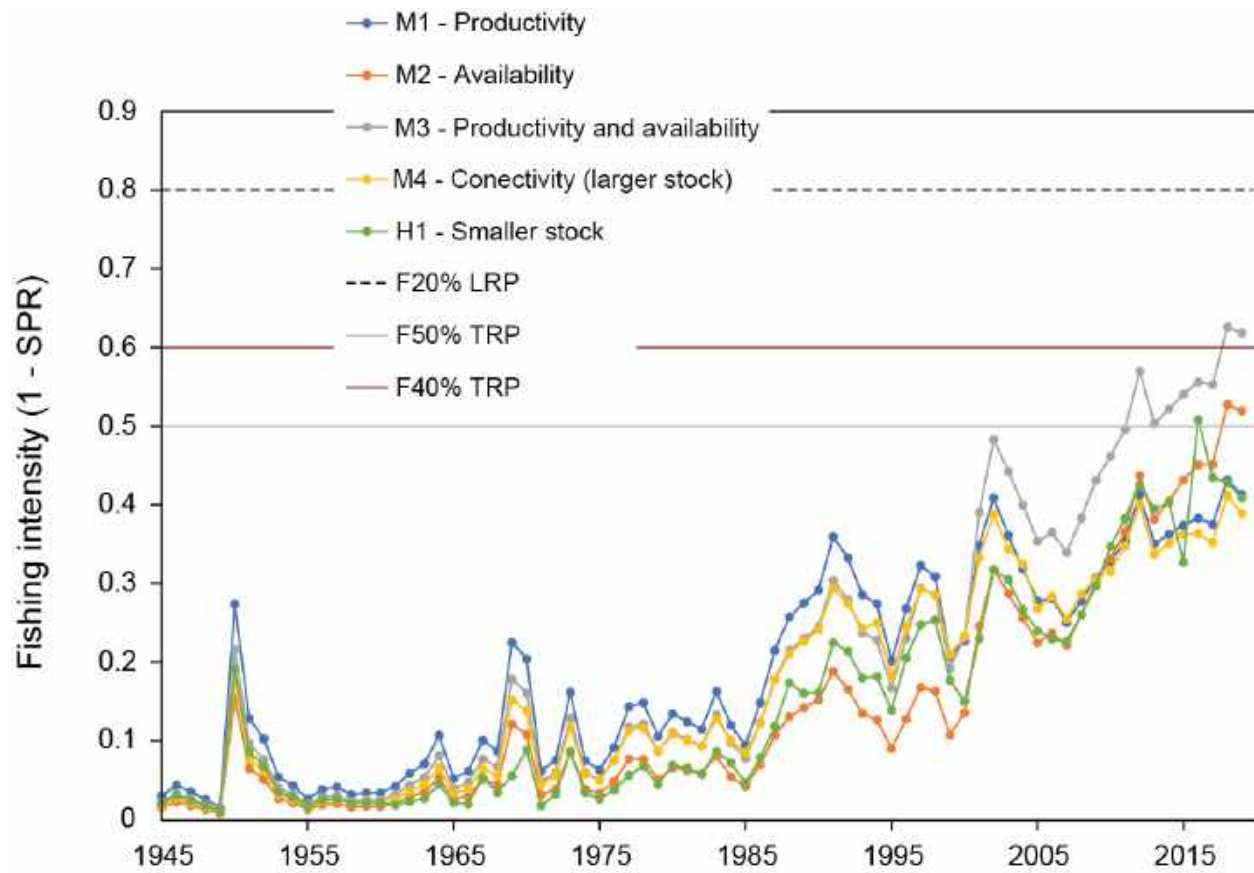


**FIGURE 18.** Fishing intensity (1-SPR) for the models corresponding to the four hypotheses that explain the simultaneous increase in indices of abundance and catches and the model corresponding to the stock structure hypothesis H1 (north boundary at 5°S). Note that M4 corresponds to the stock structure hypothesis H3 (western boundary at 170°W). Fishing intensity is a proxy for fishing mortality, based on SPR (proportion of the spawning biomass produced by each recruit with fishing relative to biomass per recruit in the unfished condition, Goodyear 1993). Large SPR are indicative of low fishing mortality, thus a proxy for fishing mortality is 1-SPR.

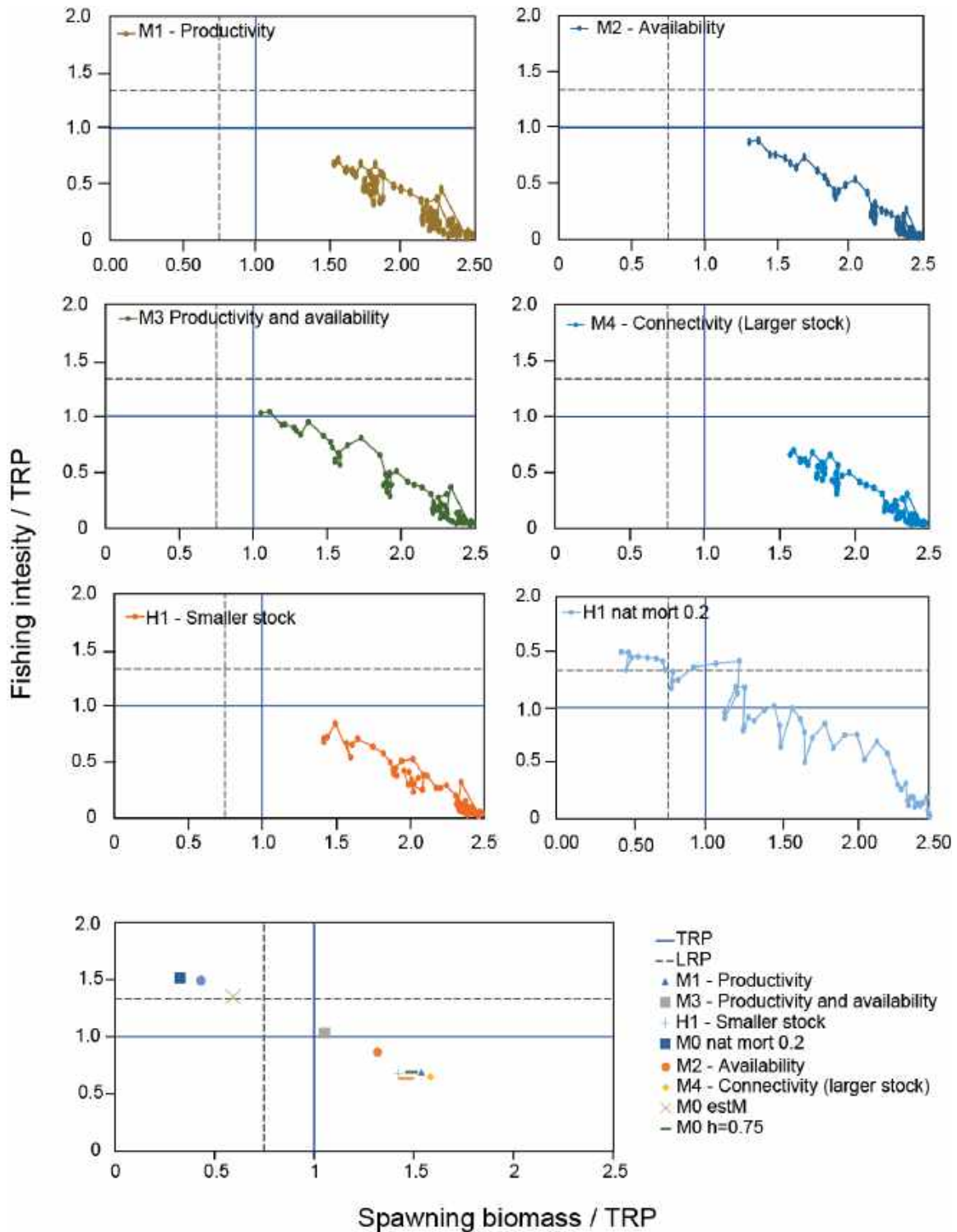


**FIGURE 19.** Phase plots: Estimated spawning biomass relative to the biomass target reference point ( $40\%SSB_{F=0}$ ) versus fishing intensity relative to the suggested target reference point ( $F40\%SPR$ ) for the models corresponding to the four hypotheses that explain the simultaneous increase in indices of abundance and catches and the model corresponding to the stock structure hypothesis H1 (north boundary at  $5^{\circ}S$ ). Note that M4 corresponds to the stock structure hypothesis H3 (western boundary at  $170^{\circ}W$ ).

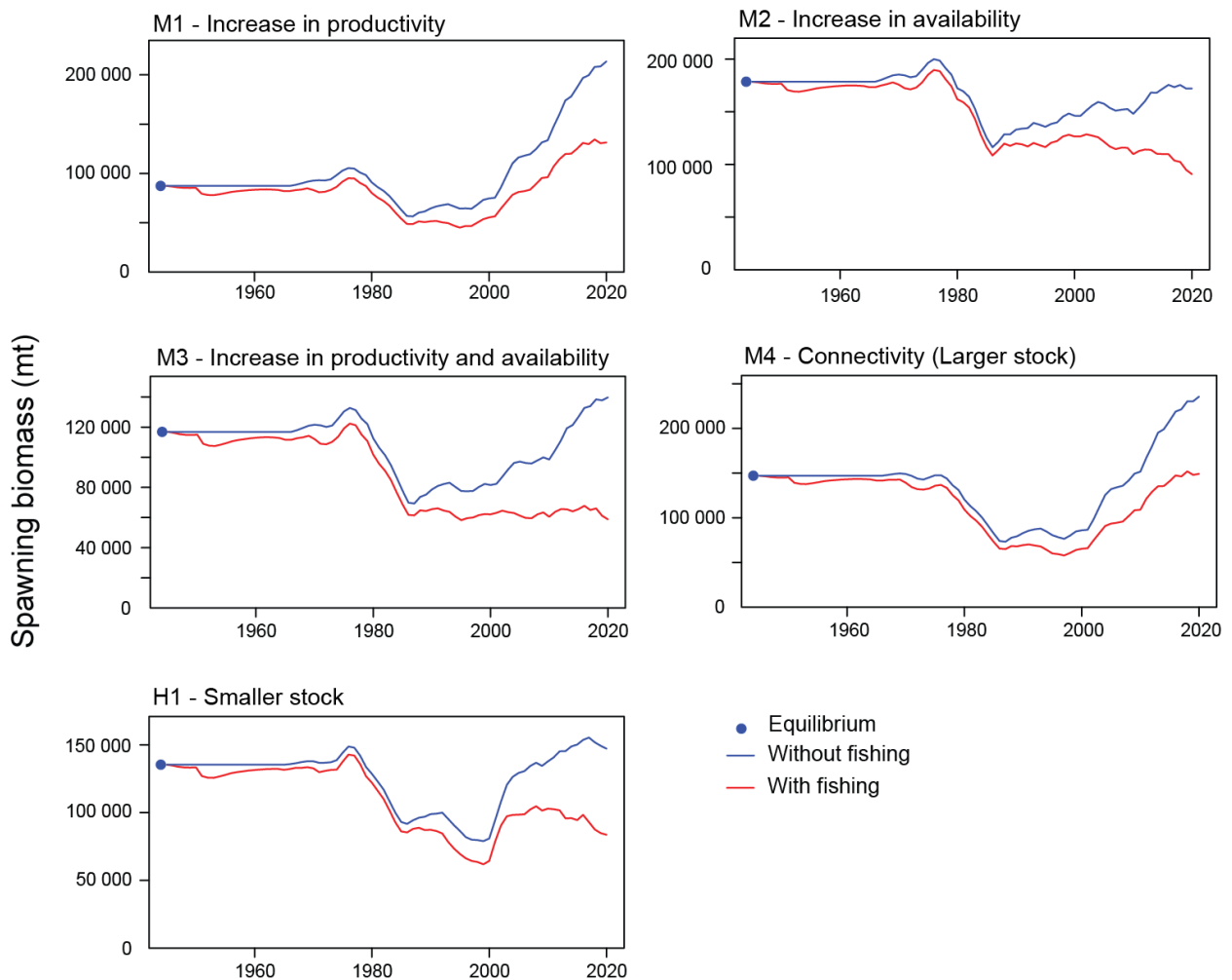


**FIGURE 20.** Fisheries impact: estimated trends in spawning biomass, with (red line) and without fishing (blue line), from fits of models corresponding to the four hypotheses that explain the simultaneous increase in indices of abundance and catches and the model corresponding to the stock structure hypothesis H1 (north boundary at 5°S). Note that M4 corresponds to the stock structure hypothesis H3 (western boundary at 170°W). The area between the red and the blue line represents the impact of the fisheries on the spawning biomass.

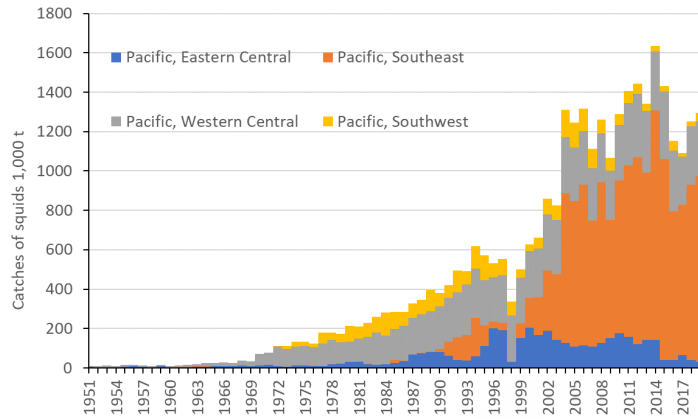


**FIGURE 21.** Catches of squids recorded at the FAO database. The main squid species targeted by fisheries in the Pacific Ocean in jumbo squid.

DRAFT

**TABLE 1.** Annual SWO catches in weight in the eastern Pacific Ocean south of 10°N (March 9<sup>th</sup>, 2022) by flag, gear and year for comparisons only. Catches in the assessment are input in the reported units. Catches for JPN in this table are an approximation done by transforming catch in numbers into weight using average weight for each area for the whole series obtained from other CPCs that report weight and numbers. JPN reports only catch in numbers in 5 by 5 by month resolution. The flag abbreviations are: CHL, Chile; COL, Colombia; CRI, Costa Rica; ECU, Ecuador; GTM, Guatemala; HDN, Honduras; NIC, Nicaragua; PAN, Panamá; PER, Perú; SLV, El Salvador; BLZ, Belize; CHN, China; JPN, Japan—Japón; KOR, Republic of Korea—República de Corea; PRT, Portugal; PYF, French Polynesia—Polinesia Francesa; TWN, Chinese Taipei— Taipei Chino, URY, Uruguay; VUT, Vanuatu; ESP, Spain—España. The gear abbreviations are: HAR – harpoon, LL - longline, GN – gillnet, OTH-other gear.

	Coastal fleets													Distant waters fleets											
	CHL GN	CHL HAR	CHL LL	COL LL	CRI LL	ECU GN	ECU LL	GTM LL	HND LL	NIC LL	PAN LL	PER GN	PER LL	SLV LL	BLZ LL	CHN LL	JPN LL	KOR LL	PRT LL	PYF LL	TWN LL	URY LL	VUT LL	ESP LL	
1945		1455																							
1946		2166																							
1947		1701																							
1948		1209																							
1949		690																							
1950		786											6969												
1951		870											2424												
1952		570											1919												
1953		416											909												
1954		334											707				21								
1955		237											404				16								
1956		386											606				10								
1957		357											606				146								
1958		392											404				112								
1959		555											404				86								
1960		456											404				148								
1961		394											303				655								
1962		297											404				1071								
1963		94											202				1897								
1964		312											909				1983					0			
1965		151											303				1230					0			
1966		175											202				1462					0			
1967		203											1313				1527					31			
1968		175											808				1668					17			
1969		314											1212				5393					6			
1970		243											2424				3449					26			
1971		181											202				2008					18			
1972		141											606				1759					38			
1973		410											1960				3237					30			
1974		218											475				2134					33			
1975		137											160				1902		10			9			
1976		13											298				2995		34			34			
1977		32											424				4237		39			31			
1978		56											440				3884		37			8			
1979		40											190				3999		37			30			
1980		104											218				3408		46			17			
1981		294											92				2999		127			35			
1982		285											156				2814		69			32			



1983		342								240			3454	60			9							
1984		103								346			1862	49			15							
1985		342								93			2488	157			12							
1986	502	245	17							33			3272	316			12							
1987	1624	245	190							74			2895	203			29							
1988	3727	245	483							130			2892	110			38							
1989	4496	245	1083							84			2404	107			111							
1990	3605	245	1105							2			2454	430			34							
1991	3041	245	3969	29	107					3			2485	586			40							
1992	2556	245	3578		27					21			5004	269		2	32							
1993	2488	245	1979		20			22		77			2598	286		2	19							
1994	2307	245	1249		27					313			2194	256		16	44							
1995	1840	245	509		29					7			1449	289		24	8							
1996	385	245	2515		315				2	1023			1447	362		25	35							
1997	718	245	3077		1072				3				2010	415		23	29		2018					
1998	1605	245	2642	6	419					99			2219	440		19	34		1302					
1999	673	245	2007		99					42			1160	351		30	81		1121					
2000	400	0	1742		407				1	192	1		2004	400		46	608		1807					
2001	1087	21	2560		653				2	450	7		316	3757	840	47	1710		3426					
2002	1258	15	2799		638					238	11		827	3469	557	4	5471		5629					
2003	1006	29	2806		286				0	320	12		982	3035	147	69	3212		5912					
2004	1697	13	1564		179				1	0	181	7	483	2139	946	48	2076	343	5607					
2005	1987	48	1946		191				0	50	2		350	1535	275	51	917		4962					
2006	1766	13	1259		444				1				350	1395	586	57	996		5152					
2007	1978	12	1874		242				0				166	1504	238	35	708	81	4730					
2008	2110	14	672		302				1	1419	2		453	1783	116	44	361	112	6717					
2009	2604	20	893		447				7		1		635	0	1	141	479	1960	628	45	549	122	8010	
2010	3280	17	1071		673				1	671	7		422	0	1	226	649	2902	669	300	43	927	208	9115
2011	4028	26	895		929				3	934	4		1376	0		510	923	3076	765	82	47	769	114	9674
2012	5168	34	1143		2205					2414	17		2784	0		847	1223	3489	1028	156	64	1024	125	8959
2013	4186	19	652		830					1494	10		1549	0		1265	1537	3182	1347		76	908	178	8466
2014	5463	13	331		1119					2211	20		1877	0		298	1531	3366	985	2	89	1158	778	8034
2015	5786	29	218		1366					1851	16		311	0		195	1958	3347	1167	509	86	1282	596	9944
2016	6972	41	478		1330	232	3243	20		29	323	459	0			55	1414	3226	1095		77	1941	290	10602
2017	7639	23	260		1250	312	2976			8	486	154	0			78	1831	2689	1289	532	104	2345	486	8902
2018	6570	23	174		1356	287	7397	6		28	230	206	0	4		78	2519	1790	836	815	170	2336	290	11405
2019	8788	16	2		1041	48	6368	5			1301	334	0	0		51	1398	1160	464	777	133	1430	770	10538
2020					598	4642										128	1440	1370	720		133	1628	803	9979

**TABLE 2.** Fisheries defined for the stock assessment of swordfish in the south EPO. Gear: HAR: harpoon; LL: longline; GN: gillnet.

**Hypothesis 1**

Fishery	Gear	Origin	Area #	Area	Quarter	Catch data	Unit	Fishery abbreviation
F1	LL	Chile	4	Coast	All	Retained catch	t	CHL_LL
F2	All	Chile + Perú	4	Coast	All	Retained catch	t	CHL + PER
F3	LL	Distant waters	3	Offshore	All	Retained catch	t	JPN + Like
F4	LL	Distant waters	4	Coast	All	Retained catch	t	JPN_Coast
F5	LL	Spain	3	Offshore	All	Retained catch	t	ESP_Off
F6	LL	Spain	4	Coast	All	Retained catch	t	ESP_Coast
F7	LL	Chile	4	Coast	All	Retained catch	1,000 s	CHL_LL_num
F8	LL	Distant waters	3	Offshore	All	Retained catch	1,000 s	JPN+Like_num
F9	LL	Distant waters	4	Coast	All	Retained catch	1,000 s	JPN_Coast_num
F10	LL	Spain	3	Offshore	All	Retained catch	1,000 s	ESP_Off_num
F11	LL	Spain	4	Coast	All	Retained catch	1,000 s	ESP_Coast_num
Survey	Gear	Origin	Area #	Area	Quarter	Period	Unit	
I1	LL	Japan	4	Coast	All	1976-1993	1,000 s	JPN_index_early_coast
I2	LL	Japan	4	Coast	All	1994-2009	1,000 s	JPN_index_mid_coast
I3	LL	Japan	4	Coast	All	2009-2019	1,000 s	JPN_index_late_coast
I4	LL	Japan	3	Offshore	All	1976-1993	1,000 s	JPN_index_early_oceanic
I5	LL	Japan	3	Offshore	All	1994-2009	1,000 s	JPN_index_mid_oceanic
I6	LL	Japan	3	Offshore	All	2009-2019	1,000 s	JPN_index_late_oceanic

**Hypotheses 2 and 3**

Fishery	Gear	Origin	Area H2	Area H3	Quarter	Catch data	Unit	Fishery abbreviation
F1	HAR	Coastal	4, 5	4, 5	All	Retained catch	t	F1_HAR
F2	GN	Coastal	4	4	All	Retained catch	t	F2_GN_A4
F3	GN	Coastal	5	5	All	Retained catch	t	F3_GN_A5
F4	LL	Coastal	4	4	All	Retained catch	t	F4_LL_Coast_A4
F5	LL	Coastal	5	5	All	Retained catch	t	F5_LL_Coast_A5
F6	LL	Spain	2	2, 6	All	Retained catch	t	F6_ESP_A2
F7	LL	Spain	3	3, 7	All	Retained catch	t	F7_ESP_A3
F8	LL	Spain	4	4	All	Retained catch	t	F8_ESP_A4
F9	LL	Spain	5	5	All	Retained catch	t	F9_ESP_A5
F10	LL	Distant waters	2	2, 6	All	Retained catch	t	F10_LL_DW_A2
F11	LL	Distant waters	3	3, 7	All	Retained catch	t	F11_LL_DW_A3
F12	LL	Distant waters	4	4	All	Retained catch	t	F12_LL_DW_A4
F13	LL	Distant waters	5	5	All	Retained catch	t	F13_LL_DW_A5
F14	LL	Spain	2	2, 6	All	Retained catch	1,000 s	F14_ESP_A2_n
F15	LL	Spain	3	3, 7	All	Retained catch	1,000 s	F15_ESP_A3_n
F16	LL	Spain	4	4	All	Retained catch	1,000 s	F16_ESP_A4_n
F17	LL	Spain	5	5	All	Retained catch	1,000 s	F17_ESP_A5_n
F18	LL	Distant waters	2	2, 6	All	Retained catch	1,000 s	F18_LL_DW_Coast_A2_n
F19	LL	Distant waters	3	3, 7	All	Retained catch	1,000 s	F19_LL_DW_Coast_A3_n
F20	LL	Distant waters	4	4	All	Retained catch	1,000 s	F20_LL_DW_Coast_A4_n
F21	LL	Distant waters	5	5	All	Retained catch	1,000 s	F21_LL_DW_Coast_A5_n
Survey	Gear	Origin	Area H2	Area H3		Period		
I1	LL	Chile	5	5	2	2000-2019	1,000 s	I1_Chile_Q2
I2	LL	Chile	5	5	3	2000-2019	1,000 s	I2_Chile_Q3
I3	LL	Japan	2-5	2-5	All	1976-1993	1,000 s	I3_JPN_early
I4	LL	Japan	2-5	2-5	All	1994-2009	1,000 s	I4_JPN_mid
I5	LL	Japan	2-5	2-5	All	2009-2019	1,000 s	I5_JPN_late
I6	LL	Spain	2-5	2-5	1	2000-2019	t	I6_ESP_Q1
I7	LL	Spain	2-5	2-5	2	2000-2019	t	I7_ESP_Q2
I8	LL	Spain	2-5	2-5	3	2000-2019	t	I8_ESP_Q3
I9	LL	Spain	2-5	2-5	4	2000-2019	t	I9_ESP_Q4

**TABLE 3.** Indices of abundance for the S EPO swordfish stock.

Flag/index abbreviation in model	Summary	Advantages	Disadvantages	Main assumptions	Ref
<b>JPN</b> I5_JPN_late I4_JPN_mid I3_JPN_early	Spatiotemporal model using R-INLA. Serie split in three due to changes in fleet strategies. Three indices obtained (1975 to 1993, 1994-2010, 2011-2019). Unit: numbers / 1000 hooks	Large spatial and temporal coverage, standardized average weight available, index derived from operational level data through collaboration with Japan.	No associated length composition, potential changes in catchability over time not removed in the standardization modelling due to lack of covariate. Indices in a broader temporal scale (year) than the model (quarter), no seasonality effect included in the standardization.	Catchability changes are well captured in the three temporal blocks, unraised fisheries length composition represent well the population.	<a href="#">SAC-13-INF-N</a>
<b>CHL</b> I1_Chile_Q2 I2_Chile_Q3	Spatiotemporal model using VAST with standardized length-frequencies (2000 – 2018). Indices for quarter 2 and quarter 3 estimated separately due to changes in spatial anisotropy by quarter. Unit: numbers / (1000 hooks)	Large sampling of length and age composition, large coverage of logbooks, index derived from fine spatial resolution (2° by 2°) from data available through collaboration with Chile.	Spatial coverage restricted to areas off the Chilean coast, effort decreased over time and fleet ceased to operate in 2019.	Well mixed stock, dynamic of the stock is captured by an index with restricted spatial coverage.	Unpublished analyses
<b>CHL</b> Not used	Generalized linear model using Tweedie distribution. Unit: number / (m <sup>2</sup> )	Large sampling of length and age composition, large coverage of logbooks, index derived from fine spatial resolution (2° by 2°) from data available through collaboration with Chile. The gillnet fleet expanded over time, and the industry is flourishing, guaranteeing the continuation of the index into the future.	Spatial coverage restricted to areas off the Chilean coast. Effort measure in area of gillnet may not fully represent the effort (which may also depend of soaking time). Index in a broader temporal scale (year) than the model (quarter), no seasonality effect included in the standardization.	Well mixed stock, dynamic of the stock is captured by an index with restricted spatial coverage.	Barraza, <i>et al</i> presentation to <a href="#">SWO-01</a>
<b>KOR</b> Not used	Spatiotemporal model including hooks-between-floats effect. Unit: numbers / (1000 hooks)	Large coverage of logbooks, index derived from fine spatial resolution (1° by 1°) through collaboration with Korea, comparison with Japanese show similar trends	Spatial coverage restricted to equatorial from 130° to the 150°W, 10°N to 15°S, far from the area where the bulk of the catches are taken.	Well mixed stock, dynamic of the stock is captured by an index with restricted spatial coverage	<a href="#">SAC-13-INF-M</a>
<b>SPN</b> I6_ESP_Q1 I7_ESP_Q2 I8_ESP_Q3 I9_ESP_Q4	Spatiotemporal model using VAST (2005-2020). Unit: kg / sets	Large coverage of logbooks, large spatial coverage of the fleet in relation to the stock distribution. Set-by-set data available through collaboration with Spain.	Only positive catches available. Catch in weight, not in numbers. Catch species composition data available for reduced area (which could allow for inclusion of target effect in the standardization model, <i>e.g.</i> Ramos-Cartelle <i>et al</i> 2021). Only number of sets available as effort measure for 2005-2017. There is indication that the number of hooks is not constant among sets or overtime (from 2018-2020 data). No gear characteristics available.	Number of hooks does not have systematic changes over time or in space. There are no other changes in the fishing strategy that may have influenced the catchability. Anisotropy invariant in space	Unpublished analyses

**TABLE 4.** Model assumptions for M0 and sensitivity models.

Structure	Assumption	Sensitivity	Reference
Starting year	1945		
End year	2019		
Starting condition	Virgin stock		
Temporal scale	Annual model with four seasons in a year		
Spatial scale	One area model, "areas-as-fleet" approach		
Sex	Sex-specific model, with sex-specific growth		
Recruitment function	Beverton-Holt model with steepness $h=1$	$h=0.75$	
Recruitment variability	0.6 .The bias correction ramp and full bias correction were estimated using a single iteration of the approach of Methot and Taylor (2011) as implemented in r4ss.		Methot and Taylor (2011)
Recruitment deviations	1964-2019 constrained to sum to zero		
Early recruitment deviations	1960-1963		
Recruitment season	1 and 2, season 2 recruitment is estimated relative to season 1		
Maturity ogive	0 for ages 1 and 1, 0.6 for age 2, 0.8 for age 3 and 1 for ages 4 and older		DeMartini et al. 2007, Claramunt et al. 2009 (based on maturity at length)
Fecundity	Equal to mature female biomass		
Natural mortality rate	0.4 -year <sup>1</sup>	0.2 year <sup>1</sup>	
Plus group	18 years (H2/H3) 15 years (H1)		
Growth	<ul style="list-style-type: none"> <li>•von Bertalanffy growth curve with fixed parameters</li> <li>•females: <math>K = 0.113</math>, <math>L_{inf} = 321</math>, size at age 1 = 118</li> <li>•males: <math>K = 0.158</math>, <math>L_{inf} = 279</math>, size at age 1 =122 cm</li> <li>•CV of age 1 = 0.10, CV of oldest age = 0.15, linear interpolation for ages in between</li> <li>•linear growth during age zero, from 10 cm to size at age 1</li> </ul>		Cerna (2009)
Eye to fork length (EFL) x Lower jaw for length (LJFL) relationship	$LJFL = 8.0084 + 1.07064 \times EFL$		Uchiyama et al. (1999)
Length- weight relationship	<ul style="list-style-type: none"> <li>•Females Weight (kg) = <math>3.7 \times 10^{-6} LJFL (cm)^{3.26}</math> ; and</li> <li>•Males Weight (kg) = <math>4.5 \times 10^{-6} \times [LJFL (cm)]^{3.21}</math></li> </ul>		Unpublished results from Francisco Cerna (IFOP-Chile)
Size structure	Population: minimum size= 10 cm, maximum size (accumulator size) 350 cm, size intervals = 1cm Data: minimum size= 50 cm, maximum size (accumulator size) 340 cm, size intervals = 10 cm; 70-270 cm, 10cm for standardized size composition for Spanish indices; 80-300 cm, 20cm for standardized size composition for Chilean indices		
Gilled and gutted weight (GG) to whole weight relationship (WW)	$WW = 1.3332 GG$ ( $n=1680$ about half females and half males, $R^2=0.9947$ )		Unpublished results from Francisco Cerna (IFOP-Chile)

**TABLE 5.** Data weighting assumptions used in the initial reference model M0 and derived models.

Likelihood component	Weighting assumption
Catches	CV=0.05
Indices	CV = 0.2 for Japanese indices (plus extra CV estimated for I4_JPN_mid) CV as estimated in the standardization model added to an estimated extra CV (except for plus I1_Chile_Q2, I2_Chile_Q3, for which it was the extra CV was fixed at 0.1)
Size and age composition	Proxy for sample size X weighting using Francis method (Francis 2011). For the standardized length composition data associated with the Spanish indices of abundance (I6_ESP_Q1, I7_ESP_Q2, I8_ESP_Q3, I9_ESP_Q4) the proxy of sample size was set to 50 (see Table 6 for final weights)

**TABLE 6.** Selectivity assumptions for the fisheries and the indices of abundance, associated composition data and composition data weighting initial reference model M0 and derived models.

Fishery abbreviation	Composition data associated	Weighting	Selectivity function at length
F1_HAR	Length	0.1	Double normal
F2_GN_A4	Length (not fitted)	0	Logistic
F3_GN_A5	Length / Age raised to the catch	0.3 / 1	Mirror F2
F4_LL_Coast_A4	Length (not fitted)	0	Double normal
F5_LL_Coast_A5	Length /Age raised to the catch	1.2 / 1.2156	Mirror F
F6_ESP_A2	Length raised to the catch	0.5	Double normal
F7_ESP_A3	Length raised to the catch	0.4	Double normal
F8_ESP_A4	Length raised to the catch	0.5	Double normal
F9_ESP_A5	Length raised to the catch	0.6	Double normal
F10_LL_DW_A2	Length	0.015	Double normal
F11_LL_DW_A3	Length	0	Mirror F10
F12_LL_DW_A4	Length	0.02307	Double normal
F13_LL_DW_A5	Length	0.026206	Double normal
F14_ESP_A2_n	None	-	Mirror F6
F15_ESP_A3_n	None	-	Mirror F7
F16_ESP_A4_n	None	-	Mirror F8
F17_ESP_A5_n	None	-	Mirror F9
F18_LL_DW_Coast_A2_n	None	-	Mirror F10
F19_LL_DW_Coast_A3_n	None	-	Mirror F11
F20_LL_DW_Coast_A4_n	None	-	Mirror F12
F21_LL_DW_Coast_A5_n	None	-	Mirror F13
Index abbreviation	Composition data associated		Selectivity function at length
I1_Chile_Q2	Standardized length using VAST	0.71254	Double normal
I2_Chile_Q3	Standardized length using VAST	0.53954	Double normal
I3_JPN_early	Length	0.05	Logistic
I4_JPN_mid	Length / Standardized average weight (R-Inla)	0.05 / 1	Spline 3 knots
I5_JPN_late	Length / Standardized average weight (R-Inla)	0.05 / 1	Spline 3 knots
I6_ESP_Q1	Standardized length using VAST	1	Double normal
I7_ESP_Q2	Standardized length using VAST	1	Double normal
I8_ESP_Q3	Standardized length using VAST	1	Double normal
I9_ESP_Q4	Standardized length using VAST	1	Double normal

**TABLE 7.** Hypotheses that explain the simultaneous increase in indices of abundance and catches in the south EPO and corresponding assessment models.

Hypothesis	Label in figures	Interpretation	Model description
1. Real increase in abundance	Productivity	There is an increasing trend in productivity due to increasing recruitment.	A regime shift in $\ln R_0$ is estimated, as a trend starting in a fixed lower productivity value ( $\ln R_0$ for a model for 1945 to 1993)
2. Increased catchability (availability)	Availability	Increasing indices may be due to a general increase in availability of the fish to all the gear. The indices do not represent the abundance of the population.	The catch curve model based on $M_0$ is estimated: The model is fit only to mean weight, age, length, and generalized size composition data. The change in availability to the indices is computed as the difference from the expected values for the indices and the observed indices
3. Increase both in abundance and availability	Productivity and availability	Factors that increase availability may also increase abundance	A model like $M_0$ is estimated, the changes in availability are obtained by estimating time-varying catchability parameters for all indices except
4. Stock structure and connectivity	Connectivity	Connectivity from the equatorial area and the southern EPO seems to have increased after 2010, perhaps connectivity between WCPO and EPO also increased.	Like $M_0$ but include the catches in the CPO (areas 6 and 7 in Figure 2 stock structure hypothesis H3)

**TABLE 8.** Support of each data component to each model measured as the difference between the negative log-likelihood for the model being analyzed and best fitting model for that data component. The components that have three or more units of maximum difference are shown in bold, except for indices of abundance with variable catchability parameter (q). For those components, the model corresponding to each of the four hypotheses with the highest support by data component is shaded in grey. M0: initial reference model, M1: Productivity, M2: Availability, M3: Productivity and availability, M4: Connectivity (Larger stock)

Data component	Fishery	M0	M1	M2	M3	M4	Maximum difference	model support, notes
Indices	I1_Chile_Q2	22.3	22.2	32.8	0.0	22.4	32.8	*
	I2_Chile_Q3	21.5	21.0	42.1	0.0	21.6	42.1	*
	I3_JPN_early	0.0	0.0	1.5	0.0	0.0	1.5	<b>M1, M3, M4, **</b>
	I4_JPN_mid	0.8	0.5	59.1	0.0	0.9	59.1	*
	I5_JPN_late	0.1	0.1	0.8	0.0	0.2	0.8	<b>M1, M3, M4, **</b>
	I6_ESP_Q1	0.0	0.7	7.2	1.6	0.1	7.2	*
	I7_ESP_Q2	0.0	0.1	5.2	1.2	0.0	5.2	*
	I8_ESP_Q3	0.0	0.1	10.1	1.9	0.2	10.1	*
	I9_ESP_Q4	0.2	0.0	25.3	3.0	0.5	25.3	*
Average weight	I4_JPN_mid	1.0	0.5	0.4	1.4	1.0	1.4	
	I5_JPN_late	0.0	0.0	0.0	0.2	0.0	0.2	
Generalized size comps	I1_Chile_Q2	2.9	3.0	0.4	0.0	3.0	<b>3.0</b>	<b>M3</b>
	I2_Chile_Q3	4.2	4.3	0.5	0.0	4.3	<b>4.3</b>	<b>M3</b>
Age comps	F3_GN_A5	1.8	2.0	0.0	7.5	1.4	<b>7.5</b>	<b>M2</b>
	F5_LL_Coast_A5	17.3	17.5	0.5	0.0	17.4	<b>17.5</b>	<b>M3</b>
Length comps	Total	30.4	31.5	0.0	23.1	31.5	<b>31.5</b>	<b>M2</b>
	F1_HAR	0.0	0.0	0.6	1.1	0.0	1.1	
	F2_GN_A4	0.0	0.0	0.1	0.1	0.0	0.1	
	F3_GN_A5	0.9	1.1	0.0	0.9	0.8	1.1	
	F4_LL_Coast_A4	0.3	0.3	0.0	0.0	0.4	0.4	
	F5_LL_Coast_A5	17.1	17.8	5.1	0.0	17.6	<b>17.8</b>	<b>M3</b>
	F6_ESP_A2	0.2	0.1	0.0	3.7	0.1	<b>3.7</b>	<b>M1, M2, M4</b>
	F7_ESP_A3	13.1	13.9	0.0	3.6	13.6	<b>13.9</b>	<b>M2</b>
	F8_ESP_A4	11.3	11.2	11.5	0.0	11.8	<b>11.8</b>	<b>M3</b>
	F9_ESP_A5	0.2	0.4	7.8	15.6	0.0	<b>15.6</b>	<b>M1, M4</b>
	F10_LL_DW_A2	6.5	5.2	0.0	5.0	6.8	<b>6.8</b>	<b>M2</b>
	F12_LL_DW_A4	0.3	0.0	3.9	1.1	0.4	<b>3.9</b>	<b>M1, M4</b>
	F13_LL_DW_A5	0.1	0.0	2.3	0.4	0.1	2.3	
	I3_JPN_early	3.9	4.4	0.0	4.3	4.0	<b>4.4</b>	<b>M2</b>
	I4_JPN_mid	7.3	8.0	0.0	3.2	7.0	<b>8.0</b>	<b>M2</b>
	I5_JPN_late	0.5	0.5	0.0	15.4	0.4	<b>15.4</b>	<b>M2, M4</b>
	I6_ESP_Q1	0.0	0.0	0.0	0.1	0.1	0.1	
	I7_ESP_Q2	0.2	0.2	0.0	0.0	0.2	0.2	
	I8_ESP_Q3	0.0	0.0	0.2	0.0	0.0	0.2	
I9_ESP_Q4	0.1	0.1	0.0	0.0	0.1	0.1		

\* Not used in M2, Variable q in M3

\*\* Not used in M2



## 11. APPENDIX 1 . Catch estimation

The catch estimation algorithm is available from [github.com/cminte/SEPO\\_SWO\\_assessment\\_2022](https://github.com/cminte/SEPO_SWO_assessment_2022)

## 12. APPENDIX 2. Early model

A model was fit to all data from 1945 to 1993. The  $\ln R_0$ , recruitment deviations and selectivities were estimated (Figure A2.1). From an ASPM based on this model the early productivity was estimated (as  $\ln R_0$ ) (Figure A2.2). This value was used in M1 as the starting productivity.

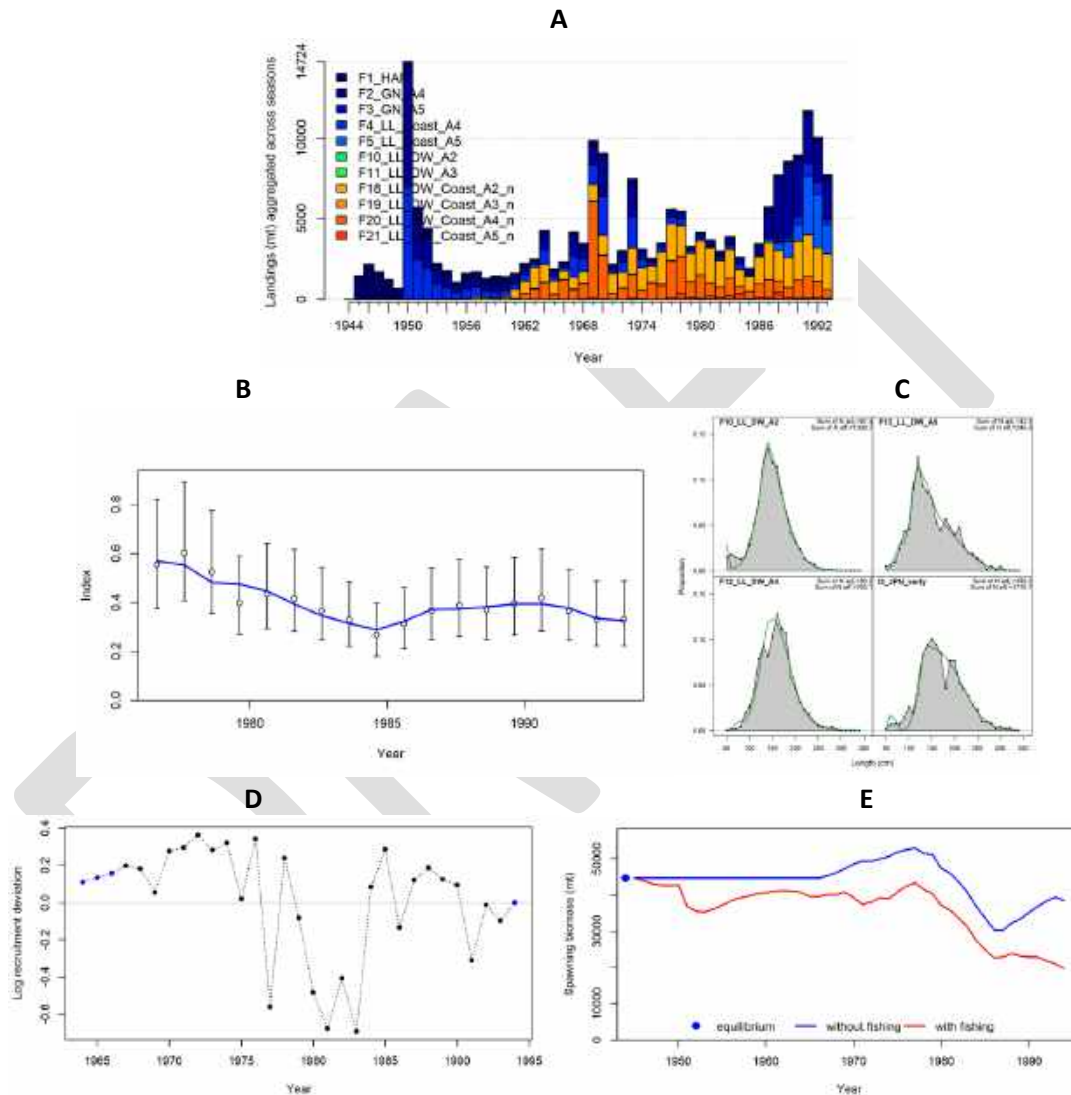


**FIGURE A2.1** Model 1: Early productivity. A: Catches, B: fit to the I3\_JPN\_early longline index, C fits to the length composition data, D: Estimates of log recruitment deviations, E: Estimated spawning biomass trajectory with and without fishing (trajectory of the spawning biomass of a simulated population of swordfish was never exploited), the area between the red and the blue lines is the impact of fishing.

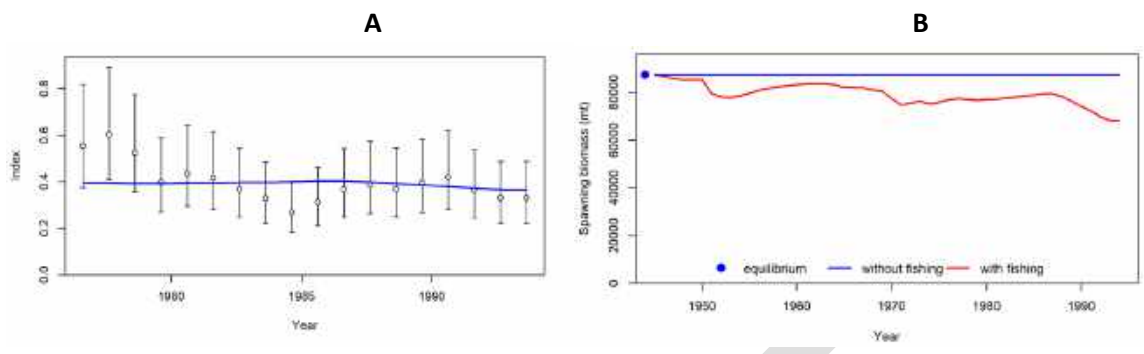


**FIGURE A2.2.** Model 2: ASPM Early productivity. **A:** fit to the I3\_JPN\_early longline index **B:** Estimated spawning biomass at equilibrium and trajectory with and without fishing

DRAFT

**APPENDIX 3 -Estimates of catchability by year for indices of abundance in model 2**

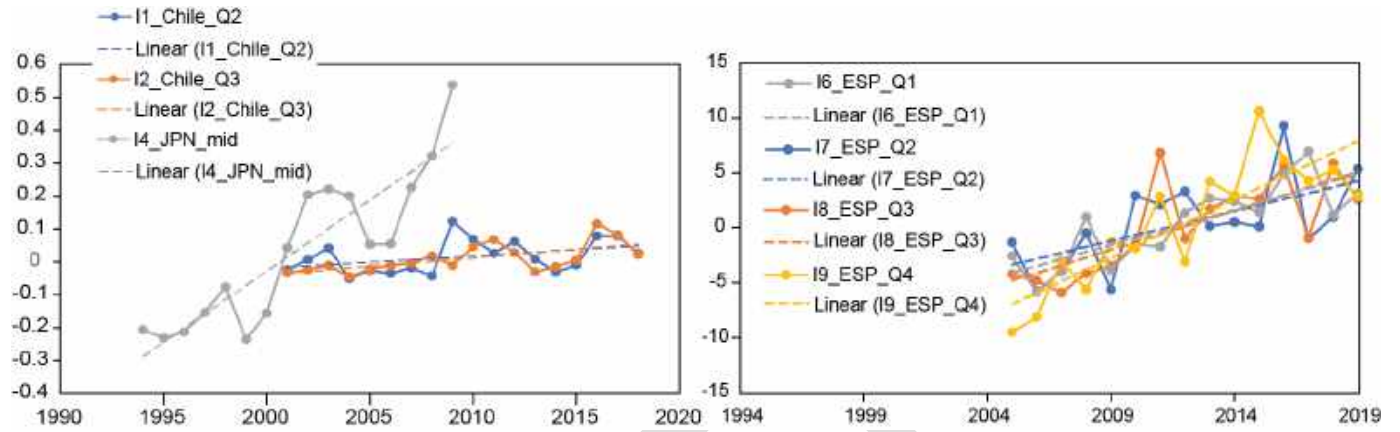


**FIGURE A3.1** Time series of estimated catchability deviations (computed as expected index – observed index) for model M2.

**APPENDIX 4. Fits to the indices of abundance of the models according to the hypotheses**

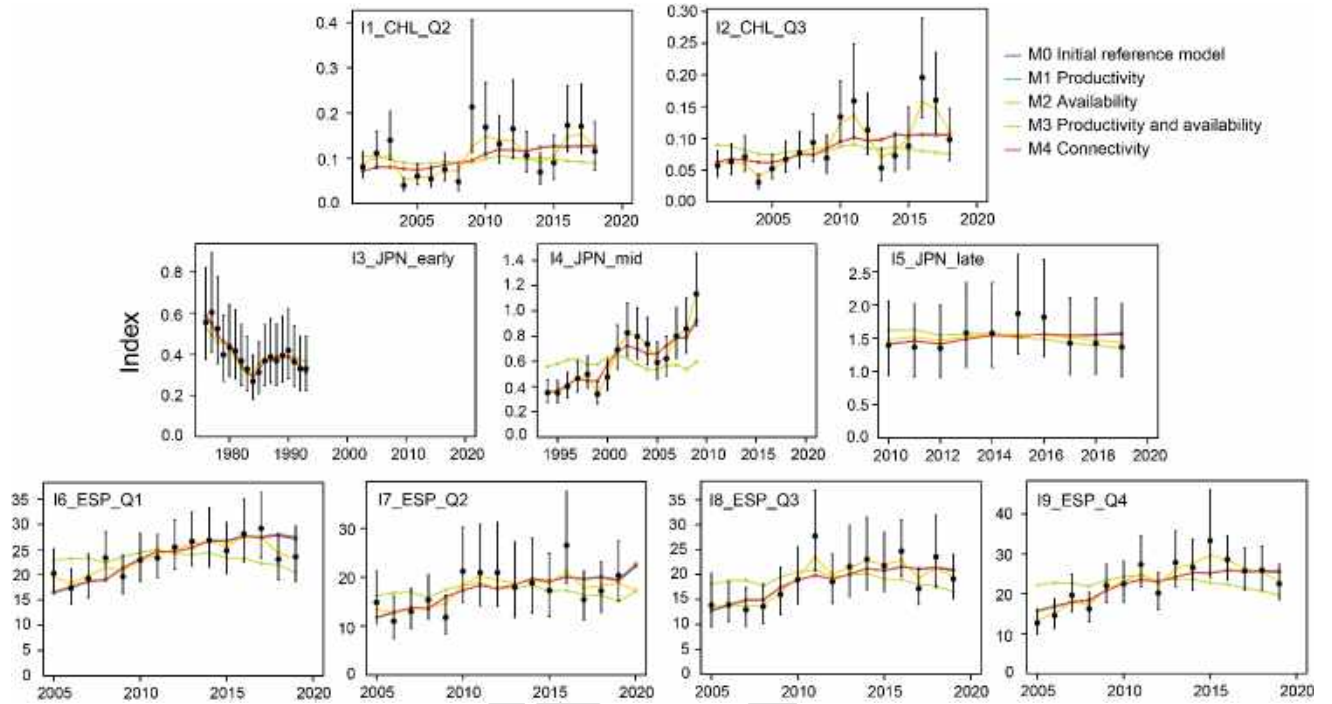


**FIGURE A4.1** Fits to the indices of abundance

DRAFT